

UNIVERSIDAD DE CONCEPCIÓN



CENTRO DE INVESTIGACIÓN EN
INGENIERÍA MATEMÁTICA (CI²MA)



Discontinuous finite volume element discretization for coupled
flow-transport problems arising in models of sedimentation

RAIMUND BÜRGER, SARVESH KUMAR,
RICARDO RUIZ-BAIER

PREPRINT 2014-25

SERIE DE PRE-PUBLICACIONES

Discontinuous finite volume element discretization for coupled flow–transport problems arising in models of sedimentation

Raimund Bürger^a, Sarvesh Kumar^b, Ricardo Ruiz-Baier^c

^a*CF²MA and Departamento de Ingeniería Matemática, Universidad de Concepción, Casilla 160-C, Concepción, Chile*

^b*Department of Mathematics, Indian Institute of Space Science and Technology, Thiruvananthapuram 695 547, Kerala, India*

^c*Institute of Earth Sciences, Géopolis UNIL-Mouline, University of Lausanne, CH-1015 Lausanne, Switzerland*

Abstract

The sedimentation-consolidation and flow processes of a mixture of small particles dispersed in a viscous fluid at low Reynolds numbers can be described by a nonlinear transport equation for the solids concentration coupled with the Stokes problem written in terms of the mixture flow velocity and the pressure field. Here both the viscosity and the forcing term depend on the local solids concentration. A continuous in time discontinuous finite volume element (DFVE) discretization for this model is proposed. The numerical method is constructed on a baseline finite element family of linear discontinuous elements for the approximation of velocity components and concentration field, whereas the pressure is approximated by piecewise constant elements. The unique solvability of both the nonlinear continuous problem and the semidiscrete DFVE scheme is discussed, and optimal convergence estimates in several spatial norms are derived. Properties of the model and the predicted space accuracy of the proposed formulation are illustrated by detailed numerical examples, including flows under gravity with changing direction, a secondary settling tank in an axisymmetric setting, and batch sedimentation in a tilted cylindrical vessel.

Key words: Discontinuous finite volume element methods, Semidiscrete scheme, Convergence to the weak solution, Error estimates, Nonlinear coupled flow and transport, Sedimentation – consolidation processes

2000 MSC: 65M60, 65M12, 65M15, 35Q35, 76D07

1. Introduction

Scope. The numerical approximation of macroscopic descriptions of sedimentation processes at low Reynolds numbers is needed in a wide variety of natural phenomena and industrial processes including wastewater treatment [6, 15], mineral processing [39], and gravity currents [37]. The governing partial differential equations typically consist in a nonlinear advection-reaction-diffusion equation for the scalar solids concentration coupled with the Stokes or Navier-Stokes problem with concentration-dependent viscosity. Despite numerous advances in handling the model complexity evidenced by the growing amount of relevant literature, most numerical methods typically employed in industry still lack essential features to reliably couple flow and transport processes. For instance, in addition to efficiency of the computational tools, it is crucial that the schemes involved be accurate and robust under various ranges

Email addresses: rburger@ing-mat.udec.cl (Raimund Bürger), sarvesh@iist.ac.in (Sarvesh Kumar), ricardo.ruizbaier@unil.ch (Ricardo Ruiz-Baier)

of model parameters and geometry configurations. Moreover, mass conservation is a key property in flow-transport problems to avoid artificial sinks or sources. Unfortunately, up to date there is no ultimate numerical tool available that would resolve all these issues at once. Some methods are easy to implement and can be readily parallelized while others are more suitable for unstructured meshes and complicated geometries, or mass conservative by construction, or allow the natural derivation of error estimates, etc. Consequently, to resolve multiphysics problems, one must resort to a scheme that combines some of the aforementioned properties.

It is the purpose of this paper to focus on one of such combined or hybrid methods, the so-called discontinuous finite volume element (DFVE) method, originally introduced for elliptic equations in [41] (see also [4, 40]), and later extended to Stokes equations in [23, 42]. This method can be seen as a combination of discontinuous Galerkin (DG) approximations and finite volume element (FVE) methods, typically regarded as Petrov-Galerkin formulations involving different trial and test spaces (see a review in [13]). Advantages of DFVE formulations include local mass conservativity, flexibility for choosing accurate numerical fluxes, smaller dual control volumes (here called diamonds), and suitability for error analysis in the L^2 -norm. In the formulation advanced in the present work, the transport equation is tested against scalar piecewise constant functions spanned by a basis associated to a diamond dual grid, the momentum equation is tested against vectorial piecewise constants also defined on the diamond mesh, and the mass conservation equation is tested against piecewise constants defined on the primal mesh. Integration by parts on each diamond of the dual mesh yields a finite volume scheme (written in terms of fluxes across dual boundaries). Then, special properties of the lumping operator connecting discrete functions defined on primal and dual meshes allow us to rewrite the formulation completely in terms of volume integrals on the primal elements, except for the mass term accompanying the time derivative of the solids concentration and the right-hand sides of both transport and momentum equations. In particular, this implies that the quantities defined on the dual mesh will be accessed only through mass and right-hand side assembly, which are typically performed just once during the entire solution algorithm.

The analysis of equivalent continuous coupled formulations can be found in [27], where the Faedo-Galerkin method is employed to establish the weak solvability of the system. Here, the well-posedness analysis of the discrete problem is based on a cut-off of the velocity combined with the properties of the transfer operator between primal and dual meshes, and Picard's Theorem. Next, classical tools consisting of energy-based methods, duality arguments, and elliptic projections are used to obtain error estimates in the natural norms for all fields.

Related work. Starting from the seminal work of Cai [9], an abundant body of recent literature is devoted to the analysis of FVE-based methods for the discretization of Stokes equations. Among these we point out that continuous approximations include, for instance, pressure-projection and multiscale stabilized methods [26, 31, 38], whereas nonconforming and discontinuous schemes include those analyzed e.g. in [12, 13, 23, 42]. Some references address the analysis of continuous FVE methods for nonlinear elliptic [11, 25] and parabolic problems [10]. DG methods have also been introduced for such kind of problems; for instance, we refer to [19, 30] and the references therein for an extensive survey on DG discretizations of nonlinear elliptic and parabolic problems. Nevertheless, and on the other hand, there are hardly any results available dealing with their DFVE counterparts.

Continuous FVE approximations (or similar concepts) have recently been introduced for coupled flow-transport problems. These include, for instance, projection-stabilized methods applied to thermal convection [28], hybrid methods for general conservation laws [16], and edge-based stabilized methods simulating sedimentation-consolidation processes in Stokes and Navier-Stokes regimes [7, 33]. However, fully discontinuous FVE methods have been only proposed and studied in the context of porous media flow, where the transport problem is usually less involved and the flow equations are governed by Darcy-like descriptions [20, 21].

The conservation property of FVE methods makes these methods more suitable for discretizing

computational fluid dynamics problems and a very little progress has been done using discontinuous functions for the finite volume setting for the approximation of nonlinear Stokes and transport problems and hence, one of the main purposes of this paper is to propose and analyze the convergence of a semidiscrete DFVE method for the approximation of coupled nonlinear Stokes and transport problems. We would like to mention that in our numerical experiments, a first order backward Euler scheme is used in order to approximate the time derivative and our analysis can be easily extended to a completely discretize scheme. To our knowledge, not even the DFVE approximation of the nonlinear transport problem alone has been addressed in the literature.

Outline. We have arranged the remainder of this paper in the following manner. Section 2 contains some basic notation and we state the governing equations, present the concept of weak solution and comment on the solvability of the continuous problem. The DFVE scheme is introduced in Section 3, and we derive optimal error estimates in Section 4. Section 5 contains several numerical results illustrating the behavior of the model, while showing the accuracy and robustness of the formulation.

2. Preliminaries and problem statement

2.1. Notation

By $\Omega \subset \mathbb{R}^d$, $d = 2, 3$ we denote a given open bounded domain with polyhedral boundary Γ , and denote by $\boldsymbol{\nu}$ the outward unit normal vector on Γ . Usual notation will be adopted for Lebesgue spaces $L^p(\Omega)$ and Sobolev spaces $H^s(\Omega)$ with norm $\|\cdot\|_{s,\Omega}$ and adopt the convention $H^0(\Omega) := L^2(\Omega)$. By \boldsymbol{M} we will denote the vectorial counterpart of the generic scalar functional space M . For a time $T > 0$, standard Bochner spaces are denoted by $L^p(0, T; H^m(\Omega))$. As usual, \boldsymbol{I} stands for the $d \times d$ identity tensor, and for any $\boldsymbol{\tau} = (\tau_{ij})_{i,j=1,\dots,d}$ and any vector field $\boldsymbol{v} = (v_i)_{i=1,\dots,d}$ we denote

$$\begin{aligned} \boldsymbol{\tau}^T &= (\tau_{ji}), \quad \text{tr}(\boldsymbol{\tau}) = \sum_{i=1}^d \tau_{ii}, \quad \boldsymbol{\tau} : \boldsymbol{\zeta} = \sum_{i,j=1}^d \tau_{ij} \zeta_{ij}, \quad \text{div } \boldsymbol{v} = \sum_{i=1}^d \partial_i v_i, \\ \text{div } \boldsymbol{\tau} &= \begin{pmatrix} \partial_1 \tau_{11} + \cdots + \partial_d \tau_{1d} \\ \vdots \\ \partial_1 \tau_{d1} + \cdots + \partial_d \tau_{dd} \end{pmatrix}, \quad \nabla \boldsymbol{v} = \begin{bmatrix} \partial_1 v_1 & \cdots & \partial_d v_1 \\ \vdots & & \vdots \\ \partial_1 v_d & \cdots & \partial_d v_d \end{bmatrix}. \end{aligned}$$

By $\mathbb{P}_k(L)$ we denote the space of polynomial functions of total degree $s \leq k$ defined on the set L . In what follows, constants independent of the meshsize will be denoted by C .

2.2. Governing equations

Let us consider a mixture occupying the domain $\Omega \subset \mathbb{R}^d$, $d = 2$ or $d = 3$. Assuming that the mixture is incompressible, we can describe the motion of the mixture and the evolution of the solids concentration by the following initial-boundary value problem:

$$\begin{aligned} \partial_t \phi - \text{div}(\kappa(\phi) \nabla \phi) + \boldsymbol{u} \cdot \nabla \phi &= \nabla \cdot \boldsymbol{f}(\phi) && \text{in } \Omega \times (0, T), \\ -\text{div}(\mu(\phi) \boldsymbol{\varepsilon}(\boldsymbol{u}) - p \boldsymbol{I}) - \phi \boldsymbol{g} &= \mathbf{0} && \text{in } \Omega \times (0, T), \\ \text{div } \boldsymbol{u} &= 0 && \text{in } \Omega \times (0, T), \\ \boldsymbol{u} &= 0 && \text{on } \Gamma \times (0, T), \\ \phi &= 0 && \text{on } \Gamma \times (0, T), \\ \phi(0) &= \phi_0 && \text{on } \Omega \times \{0\}. \end{aligned} \tag{2.1}$$

The primal unknowns are the volume average flow velocity of the mixture \boldsymbol{u} , the solids concentration ϕ , and the pressure field p . In addition, $\mu(\phi) \boldsymbol{\varepsilon}(\boldsymbol{u}) - p \boldsymbol{I}$ is the Cauchy stress tensor, $\boldsymbol{\varepsilon}(\boldsymbol{u}) = \frac{1}{2}(\nabla \boldsymbol{u} + \nabla \boldsymbol{u}^T)$

is the infinitesimal rate of strain, and $\mu = \mu(\phi)$ is the concentration-dependent viscosity, for which we assume

$$\mu \in \text{Lip}(\mathbb{R}_+); \quad \exists \mu_{\min}, \mu_{\max} > 0 : \forall s \in \mathbb{R}_+ : \mu_{\min} < \mu(s) < \mu_{\max}. \quad (2.2)$$

Moreover, the flux $\mathbf{f} = \mathbf{f}(\phi)$ is assumed to be Lipschitz continuous, and the diffusion coefficient $\kappa = \kappa(\phi)$ is a nonlinear function satisfying

$$\kappa, \kappa' \in \text{Lip}(\mathbb{R}_+); \quad \exists \gamma_1, \gamma_2, \gamma_3 > 0 : \forall x \in \mathbb{R} : \gamma_1 \leq \kappa(x) \leq \gamma_2, \quad |\kappa'(x)| \leq \gamma_3. \quad (2.3)$$

In the context of sedimentation-consolidation models, the function \mathbf{f} describes the effect of hindered settling aligned with gravity, and is usually given by $\mathbf{f}(\phi) = f_b(\phi)\mathbf{k}$, where f_b denotes the Kynch batch flux density function [5, 24] and \mathbf{k} is the upwards-pointing unit vector. The function f_b is given by

$$f_b(\phi) = \begin{cases} -v_\infty \phi V(\phi) & \text{for } 0 \leq \phi \leq \phi_{\max}, \\ 0 & \text{for } \phi < 0 \text{ or } \phi > \phi_{\max}, \end{cases}$$

where v_∞ is the Stokes velocity, that is, the settling velocity of a single particle in an unbounded fluid, ϕ_{\max} denotes a (nominal) maximum solids concentration, and $V(\phi)$ is the so-called hindered settling factor, which can for example be given by $V(\phi) = (1 - \phi/\phi_{\max})^{n_{\text{RZ}}}$, where n_{RZ} is a material-dependent exponent [32]. The function $\kappa = \kappa(\phi)$ models the combined effects of hydrodynamic self-diffusion (see [17, 18] and references cited in these works) and sediment compressibility [8]. This function is given by

$$\kappa(\phi) = D_0 - \frac{f_b(\phi)\sigma'_e(\phi)}{(\rho_s - \rho_f)g\phi},$$

where $D_0 > 0$ is the constant of hydrodynamic self-diffusion [34], ρ_s and ρ_f are the (constant) solid and fluid mass densities, respectively, and $\sigma'_e(\phi) = d\sigma_e/d\phi$ is the derivative of the so-called effective solid stress function $\sigma_e = \sigma_e(\phi)$, which characterizes sediment compressibility in the case that particles are flocculated. This function is an optional ingredient of the model, and we assume that $\sigma_e \in C^2(\mathbb{R})$ with $\sigma'_e \geq 0$. Furthermore, the forcing term $\phi\mathbf{g}$, where $\mathbf{g} = g\mathbf{k}$, models that the mixture flow is driven by local fluctuations of ϕ , and therefore of the density of the mixture, besides possible inflow and outflow conditions. Finally, as in [7, 33], we mention that a suitable choice of $\mu(\phi)$ is

$$\mu(\phi) = (1 - \phi/\tilde{\phi}_{\max})^{-\beta}, \quad (2.4)$$

where the parameter $\tilde{\phi}_{\max}$ is a second (nominal) maximum concentration. If we set $\tilde{\phi}_{\max} > \phi_{\max}$, then (2.2) is indeed satisfied.

2.3. Weak formulation

Multiplication by adequate test functions and integration by parts over Ω and using $\text{div } \mathbf{u} = 0$ yields the following weak formulation to (2.1): For $0 < t < T$, find $(\mathbf{u}(t), p(t), \phi(t)) \in \mathbf{H}_0^1(\Omega) \times L_0^2(\Omega) \times H_0^1(\Omega)$ such that

$$\begin{aligned} \langle \partial_t \phi, \varphi \rangle + A(\phi, \varphi; \phi) + C(\phi, \varphi; \mathbf{u}) - \langle \nabla \cdot \mathbf{f}(\phi), \varphi \rangle &= 0 \quad \forall \varphi \in H_0^1(\Omega), \\ \hat{A}(\mathbf{u}, \mathbf{v}; \phi) - b(\mathbf{v}, p) - d(\phi, \mathbf{v}) &= 0 \quad \forall \mathbf{v} \in \mathbf{H}_0^1(\Omega), \\ b(\mathbf{u}, q) &= 0 \quad \forall q \in L^2(\Omega), \end{aligned} \quad (2.5)$$

and $\phi(0) = \phi_0$ a.e. in Ω , where $\mathbf{H}_0^1(\Omega) := \{\mathbf{v} \in \mathbf{H}^1(\Omega) : \mathbf{v}|_\Gamma = 0\}$, $L_0^2(\Omega) := \{q \in L^2(\Omega) : \int_\Omega q \, dx = 0\}$, $H_\Gamma^1(\Omega) := \{s \in H^1(\Omega) : s|_\Gamma = 0\}$ and the involved trilinear (uppercase letters) and bilinear (lowercase) forms are defined as

$$\begin{aligned} \hat{A}(\mathbf{u}, \mathbf{v}; \phi) &:= \int_\Omega \mu(\phi) \boldsymbol{\varepsilon}(\mathbf{u}) : \boldsymbol{\varepsilon}(\mathbf{v}) \, dx, \quad A(\phi, \varphi; \psi) := \int_\Omega (\kappa(\psi) \nabla \phi) \cdot \nabla \varphi \, dx, \\ b(\mathbf{v}, q) &:= \int_\Omega q \, \text{div } \mathbf{v} \, dx, \quad C(\phi, \varphi; \mathbf{v}) = - \int_\Omega (\mathbf{v} \cdot \nabla \varphi) \phi \, dx, \quad d(\phi, \mathbf{v}) := \int_\Omega \phi \mathbf{g} \cdot \mathbf{v} \, dx, \end{aligned} \quad (2.6)$$

for all $\phi, \varphi, \psi \in H_0^1(\Omega)$, $\mathbf{u}, \mathbf{v} \in \mathbf{H}_0^1(\Omega)$, and $q \in L^2(\Omega)$.

We recall from (2.2) and (2.3) that μ, κ and κ' are Lipschitz continuous, strictly positive, and absolutely bounded functions. In addition, some stability properties of the forms defined in (2.6) are collected in the following lemma.

Lemma 2.1. *For any $\mathbf{u}, \mathbf{v}, \mathbf{w} \in \mathbf{H}^1(\Omega)$, $\phi, \varphi \in H^1(\Omega)$, $q \in L^2(\Omega)$, there exist constants $C, \beta > 0$ such that*

$$\begin{aligned} |A(\phi, \varphi; \cdot)| &\leq C \|\phi\|_{1,\Omega} \|\varphi\|_{1,\Omega}, \\ |\hat{A}(\mathbf{u}, \mathbf{v}; \cdot)| &\leq C \|\mathbf{u}\|_{1,\Omega} \|\mathbf{v}\|_{1,\Omega}, \\ |b(\mathbf{v}, q)| &\leq C \|\mathbf{v}\|_{1,\Omega} \|q\|_{0,\Omega}, \\ |d(\phi, \mathbf{v})| &\leq C \|\phi\|_{1,\Omega} \|\mathbf{v}\|_{1,\Omega}, \\ |A(\phi, \phi; \cdot)| &\geq C \|\phi\|_{1,\Omega}^2, \\ |\hat{A}(\mathbf{u}, \mathbf{u}; \cdot)| &\geq C \|\mathbf{u}\|_{1,\Omega}^2, \\ \sup_{\mathbf{v} \in \mathbf{H}_0^1(\Omega) \setminus \{0\}} \frac{b(\mathbf{v}, q)}{\|\mathbf{v}\|_{1,\Omega}} &\geq \beta \|q\|_{0,\Omega}. \end{aligned}$$

The weak solvability of the nonlinear problem (2.1) has been established in [27].

Lemma 2.2. *Let $0 \leq \phi_0 \leq \phi_{\max}$, $\phi_0 \in L^\infty(\Omega)$, and assume that $\int_0^\phi \kappa(s) ds \in L^2(0, T; H^1(\Omega))$ for $\phi \in H^1(\Omega)$. Then, there exists a unique solution to (2.5) satisfying $\phi \in L^2(0, T; H^1(\Omega)) \cap C([0, T]; L^2(\Omega))$ and $\partial_t \phi \in L^2(0, T; H^1(\Omega))$.*

3. Finite volume element discretization

3.1. A baseline FE discretization

Let \mathcal{T}_h be a regular mesh of Ω formed by closed triangular (tetrahedral if $d = 3$) elements K with boundary ∂K and diameter h_K and by vertices $s_j, j = 1, \dots, N_h$. Each face σ between two neighboring elements K and L has diameter h_σ . The set of all faces in \mathcal{T}_h is denoted by \mathcal{E}_h , and \mathcal{E}_h^Γ is its restriction to boundary faces.

Associated to the mesh \mathcal{T}_h with meshsize $h := \max_{K \in \mathcal{T}_h} (h_K)$ we define the finite element spaces

$$\begin{aligned} \mathcal{V}_h &:= \{\mathbf{v} \in \mathbf{L}^2(\Omega) : \mathbf{v}|_K \in \mathbb{P}_1(K)^d, \forall K \in \mathcal{T}_h\}, \quad \mathcal{Q}_h := \{q \in L_0^2(\Omega) : q|_K \in \mathbb{P}_0(K), \forall K \in \mathcal{T}_h\}, \\ \mathcal{S}_h &:= \{\varphi \in L^2(\Omega) : \varphi|_K \in \mathbb{P}_1(K), \forall K \in \mathcal{T}_h\} \end{aligned}$$

for the approximation of the velocity \mathbf{v} , the pressure p and the concentration ϕ , respectively.

Let $\mathbf{n}_{K,\sigma}$ denote the outward vector of $K \in \mathcal{T}_h$ normal to $\sigma \subset \partial K$. For a scalar function $q \in L^2(\Omega)$ we let $\llbracket q \rrbracket_\sigma := q|_{\partial K} \mathbf{n}_{K,\sigma} + q|_{\partial L} \mathbf{n}_{L,\sigma}$ denote a vector jump across the face $\sigma = \bar{K} \cap \bar{L}$ and $\{q\}_\sigma$ denotes its average value on σ . If $\sigma \in \mathcal{E}_h^\Gamma$, then we simply consider $\llbracket q \rrbracket_\sigma = \{q\}_\sigma = q|_\sigma$.

3.2. Statement of the FVE method and technical results

We define a FVE discretization of the governing equations on Ω following [7, 20, 42]. To this end, we introduce a so-called diamond mesh \mathcal{T}_h^\sharp consisting of diamonds D_σ generated by barycentric subdivision, which means that each diamond $D_\sigma \in \mathcal{T}_h^\sharp$ is associated to the face $\sigma \in \mathcal{E}_h$ and constructed by joining the barycenters b_K and b_L of the elements K and L sharing the interior face σ , with the vertices of σ .

The transfer between meshes represents a projection of the FE spaces for the approximation of velocity and concentration defined above, on the following finite-dimensional spaces:

$$\begin{aligned}\mathbf{V}_h^\sharp &:= \{ \mathbf{v} \in \mathbf{L}^2(\Omega) : \mathbf{v}|_{D_\sigma} \in \mathbb{P}_0(D_\sigma)^d, \forall D_\sigma \in \mathcal{T}_h^\sharp \}, \\ \mathcal{S}_h^\sharp &:= \{ \varphi \in L^2(\Omega) : \varphi|_{D_\sigma} \in \mathbb{P}_0(D_\sigma), \forall D_\sigma \in \mathcal{T}_h^\sharp \}.\end{aligned}$$

In order to connect \mathbf{V}_h to \mathbf{V}_h^\sharp and \mathcal{S}_h to \mathcal{S}_h^\sharp , respectively, we define the projection maps $\mathcal{P}^\sharp : \mathbf{V}_h \rightarrow \mathbf{V}_h^\sharp$ and $\mathcal{R}^\sharp : \mathcal{S}_h \rightarrow \mathcal{S}_h^\sharp$ as follows:

$$\mathcal{P}^\sharp \mathbf{v}|_{D_\sigma} = \frac{1}{h_\sigma} \int_\sigma \mathbf{v}|_{D_\sigma} \, ds, \quad \mathcal{R}^\sharp \psi|_{D_\sigma} = \frac{1}{h_\sigma} \int_\sigma \psi|_{D_\sigma} \, ds, \quad D_\sigma \in \mathcal{T}_h^\sharp.$$

The construction of the dual mesh D_σ enables us to state the following technical lemma, which formulates the properties of these operators (see proofs in e.g. [20, 22]):

Lemma 3.1. *Let $\mathbf{v}_h \in \mathbf{V}_h, \varphi_h, \psi_h \in \mathcal{S}_h$, with ψ_h also in $H^2(K)$, and let $K \in \mathcal{T}_h$ and $\sigma \subset \partial K$. Then the following properties are satisfied:*

$$\int_\sigma (\varphi_h - \mathcal{R}^\sharp \varphi_h) \, ds = 0, \quad \int_\sigma (\mathbf{v}_h - \mathcal{P}^\sharp \mathbf{v}_h) \, ds = 0, \quad (3.1)$$

$$\int_K (\varphi_h - \mathcal{R}^\sharp \varphi_h) \, ds = 0, \quad \int_K (\mathbf{v}_h - \mathcal{P}^\sharp \mathbf{v}_h) \, ds = 0, \quad (3.2)$$

$$\|\mathbf{v}_h - \mathcal{P}^\sharp \mathbf{v}_h\|_{0,K} \leq Ch_K |\mathbf{v}_h|_{1,K}, \quad \|\varphi_h - \mathcal{R}^\sharp \varphi_h\|_{0,K} \leq Ch_K |\varphi_h|_{1,K}, \quad (3.3)$$

$$[[\psi_h]]_\sigma = \mathbf{0} \Rightarrow [[\mathcal{R}^\sharp \psi_h]]_\sigma = \mathbf{0}, \quad [[\mathbf{v}_h]]_\sigma = \mathbf{0} \Rightarrow [[\mathcal{P}^\sharp \mathbf{v}_h]]_\sigma = \mathbf{0}, \quad (3.4)$$

$$\int_\sigma |(\varphi_h - \mathcal{R}^\sharp \varphi_h)| \, ds \leq Ch \|\psi\|_{p,K} \|\varphi_h\|_{p'}, \quad \forall \psi \in H_p^1(K), \quad \varphi_h \in \mathcal{S}_h, \quad \frac{1}{p} + \frac{1}{p'} = 1. \quad (3.5)$$

For our future analysis we also define the following mesh-dependent norms for all $\psi_h \in \mathcal{S}(h) := \mathcal{S}_h + (H^2(\Omega) \cap H_0^1(\Omega))$ and $\mathbf{v}_h \in \mathbf{V}(h) := \mathbf{V}_h + (\mathbf{H}^2(\Omega) \cap \mathbf{H}_0^1(\Omega))$:

$$\begin{aligned}\|\psi_h\|_h^2 &:= \sum_{K \in \mathcal{T}_h} \|\nabla \psi_h\|_{0,K}^2 + \sum_{\sigma \in \mathcal{E}_h} h_\sigma^{-1} \|[[\psi_h]]_\sigma\|_{0,\sigma}^2, \quad \|\psi_h\|^2 := \|\psi_h\|_h^2 + \sum_{K \in \mathcal{T}_h} h_K^2 |\psi_h|_{2,K}^2, \\ \|\mathbf{v}_h\|_h^2 &:= \sum_{K \in \mathcal{T}_h} |\mathbf{v}_h|_{1,K}^2 + \sum_{\sigma \in \mathcal{E}_h} h_\sigma^{-1} \|[[\mathbf{v}_h]]_\sigma\|_{0,\sigma}^2.\end{aligned}$$

The standard inequality implies that there exists $C > 0$ such that

$$\|\varphi_h\| \leq C \|\varphi_h\|_h \quad \forall \varphi_h \in \mathcal{S}_h.$$

We will also make use of the following well-established trace inequalities (cf. [1, Th. 3.10]):

$$\begin{aligned}\|\mathbf{v}\|_{0,\sigma}^2 &\leq C(h_K^{-1} \|\mathbf{v}\|_{0,K}^2 + h_K |\mathbf{v}|_{1,K}^2) \quad \forall \mathbf{v} \in \mathbf{H}^1(K), \\ \|(\nabla \mathbf{v}) \mathbf{n}_{K,\sigma}\|_{0,\sigma}^2 &\leq C(h_K^{-1} |\mathbf{v}|_{1,K}^2 + h_K |\mathbf{v}|_{2,K}^2) \quad \forall \mathbf{v} \in \mathbf{H}^2(K)\end{aligned} \quad (3.6)$$

for $\sigma \subset \partial K$, where $C > 0$ depends also on the minimum angle of $K \in \mathcal{T}_h$.

Let $\varphi_h \in \mathcal{S}_h, \mathbf{v}_h \in \mathbf{V}_h, q_h \in \mathcal{Q}_h$ be suitable test functions. We proceed to multiply the concentration and momentum equations by $\mathcal{R}^\sharp \varphi_h \in \mathcal{S}_h^\sharp$ and $\mathcal{P}^\sharp \mathbf{v}_h \in \mathbf{V}_h^\sharp$, respectively, and integrating by parts the respective results over each diamond $D_\sigma \in \mathcal{T}_h^\sharp$; and to multiply the mass conservation equation by q_h and integrating by parts the result over $K \in \mathcal{T}_h$. Adding the resulting local conservation equations we

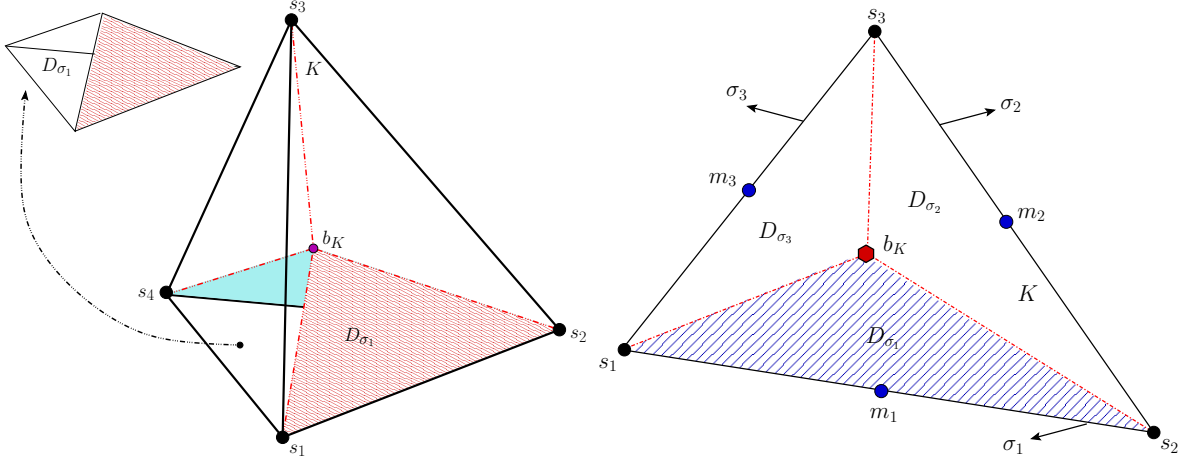


Figure 1: Left: Tetrahedral element $K \in \mathcal{T}_h$ (solid lines) with barycenter b_K , subdivided into four diamonds D_{σ_j} (dashed lines), where D_{σ_1} is highlighted for sake of visualization. Right: Two-dimensional counterpart, including also the three midpoints m_j of each edge σ_j .

end up with a variational formulation written in the form: Find (ϕ, \mathbf{u}, p) such that

$$\begin{aligned}
\langle \partial_t \phi, \mathcal{R}^\# \varphi_h \rangle - \sum_{D_\sigma \in \mathcal{T}_h^\#} \int_{\partial D_\sigma} [\kappa(\phi) \nabla \phi - \phi \mathbf{u}] \cdot \mathbf{n} \mathcal{R}^\# \varphi_h \, ds &= \sum_{D_\sigma \in \mathcal{T}_h^\#} \int_{\partial D_\sigma} \mathbf{f}(\phi) \cdot \mathbf{n} \mathcal{R}^\# \varphi_h \, ds \quad \forall \varphi_h \in \mathcal{S}_h, \\
- \sum_{D_\sigma \in \mathcal{T}_h^\#} \int_{\partial D_\sigma} \mu(\phi) \varepsilon(\mathbf{u}) \mathbf{n} \cdot \mathcal{P}^\# \mathbf{v}_h \, ds + \sum_{D_\sigma \in \mathcal{T}_h^\#} \int_{\partial D_\sigma} p \mathbf{n} \cdot \mathcal{P}^\# \mathbf{v}_h \, ds &= d(\phi, \mathcal{P}^\# \mathbf{v}_h) \quad \forall \mathbf{v}_h \in \mathcal{V}_h, \\
b(\mathbf{u}, q_h) &= 0 \quad \forall q_h \in \mathcal{Q}_h.
\end{aligned} \tag{3.7}$$

Now let $D_{\sigma_j} \in \mathcal{T}_h^\#$, with $j = 1, \dots, d+1$, be the $d+1$ sub-elements (triangles if $d = 2$, or tetrahedra if $d = 3$) contained in element K of the primal mesh \mathcal{T}_h , as sketched in Figure 1. It follows that

$$\begin{aligned}
\sum_{D_\sigma \in \mathcal{T}_h^\#} \int_{\partial D_\sigma} [\kappa(\phi) \nabla \phi - \phi \mathbf{u}] \cdot \mathbf{n} \mathcal{R}^\# \varphi_h \, ds &= \sum_{K \in \mathcal{T}_h} \sum_{j=1}^{d+1} \int_{\partial D_{\sigma_j}} [\kappa(\phi) \nabla \phi - \phi \mathbf{u}] \cdot \mathbf{n} \mathcal{R}^\# \varphi_h \, ds \\
&= \sum_{K \in \mathcal{T}_h} \sum_{j=1}^{d+1} \int_{s_{j+1} b_K s_j} (\kappa(\phi) \nabla \phi - \phi \mathbf{u}) \cdot \mathbf{n} \mathcal{R}^\# \varphi_h \, ds \\
&\quad + \sum_{K \in \mathcal{T}_h} \int_{\partial K} (\kappa(\phi) (\nabla \phi) - \phi \mathbf{u} \cdot \mathbf{n}) \mathcal{R}^\# \varphi_h \, ds
\end{aligned}$$

where $s_{d+2} = s_1$. Similarly, we can assert that

$$\begin{aligned}
\sum_{D_\sigma \in \mathcal{T}_h^\#} \int_{\partial D_\sigma} \mu(\phi) \varepsilon(\mathbf{u}) \mathbf{n} \cdot \mathcal{P}^\# \mathbf{v}_h \, ds &= \sum_{K \in \mathcal{T}_h} \sum_{j=1}^{d+1} \int_{s_{j+1} b_K s_j} \mu(\phi) \varepsilon(\mathbf{u}) \mathbf{n} \cdot \mathcal{P}^\# \mathbf{v}_h \, ds \\
&\quad + \sum_{K \in \mathcal{T}_h} \int_{\partial K} \mu(\phi) \varepsilon(\mathbf{u}) \mathbf{n} \cdot \mathcal{P}^\# \mathbf{v}_h \, ds, \\
\sum_{D_\sigma \in \mathcal{T}_h^\#} \int_{\partial D_\sigma} p \mathbf{n} \cdot \mathcal{P}^\# \mathbf{v}_h \, ds &= \sum_{K \in \mathcal{T}_h} \sum_{j=1}^{d+1} \int_{s_{j+1} b_K s_j} p \mathbf{n} \cdot \mathcal{P}^\# \mathbf{v}_h \, ds + \sum_{K \in \mathcal{T}_h} \int_{\partial K} p \mathbf{n} \cdot \mathcal{P}^\# \mathbf{v}_h \, ds,
\end{aligned}$$

$$\begin{aligned} \sum_{D_\sigma \in \mathcal{T}_h^\#} \int_{\partial D_\sigma} \mathbf{f}(\phi) \cdot \mathbf{n} \mathcal{R}^\# \varphi_h \, ds &= \sum_{K \in \mathcal{T}_h} \sum_{j=1}^{d+1} \int_{s_{j+1} b_K s_j} \mathbf{f}(\phi) \cdot \mathbf{n} \mathcal{R}^\# \varphi_h \, ds \\ &+ \sum_{K \in \mathcal{T}_h} \int_{\partial K} \mathbf{f}(\phi) \cdot \mathbf{n} \mathcal{R}^\# \varphi_h \, ds. \end{aligned}$$

Let us next define the following forms for all $\psi_h, \varphi_h, \chi_h \in \mathcal{S}_h$, $\mathbf{w}_h, \mathbf{v}_h \in \mathcal{V}_h$ and $r_h, q_h \in \mathcal{Q}_h$:

$$\begin{aligned} \mathcal{A}_h^1(\psi_h, \varphi_h; \chi_h, \mathbf{v}_h) &:= - \sum_{K \in \mathcal{T}_h} \sum_{j=1}^{d+1} \int_{s_{j+1} b_K s_j} (\kappa(\chi_h) \nabla \psi_h - \psi_h \mathbf{v}_h) \cdot \mathbf{n} \mathcal{R}^\# \varphi_h \, ds, \\ \hat{\mathcal{A}}_h^1(\mathbf{w}_h, \mathbf{v}_h; \psi_h) &:= - \sum_{K \in \mathcal{T}_h} \sum_{j=1}^{d+1} \int_{s_{j+1} b_K s_j} \mu(\psi_h) \boldsymbol{\varepsilon}(\mathbf{w}_h) \mathbf{n} \cdot \mathcal{P}^\# \mathbf{v}_h \, ds, \\ c_h^1(\mathbf{v}_h, r_h) &:= \sum_{K \in \mathcal{T}_h} \sum_{j=1}^{d+1} \int_{s_{j+1} b_K s_j} r_h \mathbf{n} \cdot \mathcal{P}^\# \mathbf{v}_h \, ds, \\ l_h^1(\psi_h; \varphi_h) &:= \sum_{K \in \mathcal{T}_h} \sum_{j=1}^{d+1} \int_{s_{j+1} b_K s_j} \mathbf{f}(\psi_h) \cdot \mathbf{n} \mathcal{R}^\# \varphi_h \, ds. \end{aligned}$$

Regularity assumptions on the exact solutions to the continuous problem imply, in particular, that

$$[[\kappa(\phi)(\nabla \phi \cdot \mathbf{n})]]_\sigma = 0, \quad [[\mu(\phi) \boldsymbol{\varepsilon}(\mathbf{u}) \mathbf{n}]]_\sigma = 0, \quad [[\phi(\mathbf{u} \cdot \mathbf{n})]]_\sigma = 0, \quad \text{and} \quad [[p]]_\sigma = 0.$$

Then, using definitions of sums and averages and integration by parts, we can rewrite the integrals initially defined on the elements boundary ∂K , in terms of $[[\cdot]]_\sigma$ and $\{\cdot\}_\sigma$. This derivation yields the following semidiscrete DFVE formulation associated to the weak formulation (3.7): For all $0 < t < T$, find $(\phi_h(t), \mathbf{u}_h(t), p_h(t)) \in \mathcal{S}_h \times \mathcal{V}_h \times \mathcal{Q}_h$ such that

$$\langle \partial_t \phi_h, \mathcal{R}^\# \varphi_h \rangle + \mathcal{A}_h(\phi_h(t), \varphi_h; \phi_h(t), \mathbf{u}_h(t)) = l_h(\phi_h(t); \varphi_h) \quad \forall \varphi_h \in \mathcal{S}_h, \quad (3.8)$$

$$\hat{\mathcal{A}}_h(\mathbf{u}_h(t), \mathbf{v}_h; \phi_h(t)) + c_h(\mathbf{v}_h, p_h(t)) = d(\phi_h(t), \mathcal{P}^\# \mathbf{v}_h) \quad \forall \mathbf{v}_h \in \mathcal{V}_h, \quad (3.9)$$

$$b_h(\mathbf{u}_h(t), q_h) = 0 \quad \forall q_h \in \mathcal{Q}_h, \quad (3.10)$$

where we define

$$\begin{aligned} \mathcal{A}_h(\psi_h, \varphi_h; \chi_h, \mathbf{w}_h) &:= \mathcal{A}_h^1(\psi_h, \varphi_h; \chi_h, \mathbf{w}_h) - \sum_{\sigma \in \mathcal{E}_h} \int_\sigma \{(\kappa(\chi_h) \nabla \psi_h - \psi_h \mathbf{w}_h) \cdot \mathbf{n}\}_\sigma \cdot [[\mathcal{R}^\# \varphi_h]]_\sigma \, ds \\ &- \sum_{\sigma \in \mathcal{E}_h} \int_\sigma \{\kappa(\chi_h) (\nabla \varphi_h \cdot \mathbf{n})\}_\sigma \cdot [[\mathcal{R}^\# \psi_h]]_\sigma \, ds + \sum_{\sigma \in \mathcal{E}_h} \int_\sigma \frac{\alpha_c}{h_\sigma} [[\psi_h]]_\sigma \cdot [[\varphi_h]]_\sigma \, ds, \\ \hat{\mathcal{A}}_h(\mathbf{w}_h, \mathbf{v}_h; \psi_h) &:= \hat{\mathcal{A}}_h^1(\mathbf{w}_h, \mathbf{v}_h; \psi_h) - \sum_{\sigma \in \mathcal{E}_h} \int_\sigma \{\mu(\psi_h) \boldsymbol{\varepsilon}(\mathbf{w}_h) \mathbf{n}\}_\sigma \cdot [[\mathcal{P}^\# \mathbf{v}_h]]_\sigma \, ds \\ &- \sum_{\sigma \in \mathcal{E}_h} \int_\sigma \{\mu(\psi_h) \boldsymbol{\varepsilon}(\mathbf{v}_h) \mathbf{n}\}_\sigma \cdot [[\mathcal{P}^\# \mathbf{w}_h]]_\sigma \, ds + \sum_{\sigma \in \mathcal{E}_h} \int_\sigma \frac{\alpha_d}{h_\sigma} [[\mathbf{w}_h]]_\sigma \cdot [[\mathbf{v}_h]]_\sigma \, ds, \\ l_h(\psi_h; \varphi_h) &:= l_h^1(\psi_h; \varphi_h) + \sum_{\sigma \in \mathcal{E}_h} \int_\sigma \{\mathbf{f}(\psi_h) \cdot \mathbf{n}\}_\sigma [[\varphi_h]]_\sigma \, ds, \\ c_h(\mathbf{v}_h, r_h) &:= c_h^1(\mathbf{v}_h, r_h) + \sum_{\sigma \in \mathcal{E}_h} \int_\sigma \{r_h\}_\sigma [[\mathbf{v}_h]]_\sigma \, ds, \\ b_h(\mathbf{w}_h, q_h) &:= b(\mathbf{w}_h, q_h) - \sum_{\sigma \in \mathcal{E}_h} \int_\sigma \{q_h\}_\sigma [[\mathbf{w}_h]]_\sigma \, ds. \end{aligned}$$

A simple application of the Gauss divergence theorem provides the following relation.

Lemma 3.2. *The following relations hold for all $\psi_h, \varphi_h, \chi_h \in \mathcal{S}_h$, $\mathbf{w}_h, \mathbf{v}_h \in \mathcal{V}_h$, and $q_h \in \mathcal{Q}_h$.*

$$\begin{aligned}
-A(\psi_h, \varphi_h; \chi_h) &= \sum_{K \in \mathcal{T}_h} \sum_{j=1}^{d+1} \int_{s_{j+1} b_K s_j} (\kappa(\chi_h) \nabla \psi_h) \cdot \mathbf{n} \mathcal{R}^\# \varphi_h \, ds \\
&\quad + \sum_{K \in \mathcal{T}_h} \int_{\partial K} (\kappa(\chi_h) \nabla \psi_h) \cdot \mathbf{n} (\mathcal{R}^\# \varphi_h - \varphi_h) \, ds \\
&\quad + \sum_{K \in \mathcal{T}_h} \int_K \nabla \cdot (\kappa(\chi_h) \nabla \psi_h) (\varphi_h - \mathcal{R}^\# \varphi_h) \, dx,
\end{aligned} \tag{3.11}$$

$$\begin{aligned}
\hat{A}_h^1(\mathbf{w}_h, \mathbf{v}_h; \psi_h) &= \hat{A}(\mathbf{w}_h, \mathbf{v}_h; \psi_h) + \sum_{K \in \mathcal{T}_h} \int_{\partial K} \mu(\psi_h) (\mathcal{P}^\# \mathbf{v}_h - \mathbf{v}_h) \boldsymbol{\varepsilon}(\mathbf{w}_h) : \mathbf{n} \, ds \\
&\quad + \sum_{K \in \mathcal{T}_h} \int_K \nabla \cdot (\mu(\psi_h) \boldsymbol{\varepsilon}(\mathbf{w}_h)) \cdot (\mathbf{v}_h - \mathcal{P}^\# \mathbf{v}_h) \, dx,
\end{aligned} \tag{3.12}$$

$$c_h^1(\mathbf{v}_h, q_h) = -b(\mathbf{v}_h, q_h). \tag{3.13}$$

PROOF. Relations (3.11) and (3.12) follow as in [41, p. 1067], whereas (3.13) can be established using [42, p. 189].

4. Solvability and convergence analysis

4.1. Solvability

Let us define the following “cut-off” operator \mathcal{N} for the velocity (see [35]):

$$\mathcal{N}(\mathbf{u})(x) := \min\{|\mathbf{u}(x)|, N\} \frac{\mathbf{u}(x)}{|\mathbf{u}(x)|},$$

where N is a fixed positive number and $|\mathbf{u}(x)| = (\sum_{i=1}^d u_i(x)^2)^{1/2}$. The map \mathcal{N} is uniformly bounded and uniformly Lipschitz continuous (see [35, p. 331]), i.e.,

$$\|\mathcal{N}(\mathbf{u}) - \mathcal{N}(\mathbf{v})\|_{\infty, \Omega} \leq \|\mathbf{u} - \mathbf{v}\|_{\infty, \Omega}. \tag{4.1}$$

For now on let us denote $\mathcal{N}(\mathbf{u}_h)(x)$ as \mathbf{u}_h^N . It is still left to precisely define this “cut-off” operator, but for the moment it suffices to note that in the subsequent analysis we will require the computed velocity \mathbf{u}_h to be uniformly bounded, which can be guaranteed by the definition of \mathcal{N} .

Using (3.11), (3.1), (3.2) and following the lines in the proof of [22, Lemma 2.3], it is not hard to prove that the bilinear form $\hat{A}_h(\cdot, \cdot; \phi_h)$ (for a fixed ϕ_h) is coercive with respect to $\|\cdot\|_h$, i.e., there exists a positive constant α independent of the mesh size h such that

$$\hat{A}_h(\mathbf{v}_h, \mathbf{v}_h; \phi_h) \geq \alpha \|\mathbf{v}_h\|_h^2.$$

Moreover, the choice of finite element spaces \mathcal{V}_h and \mathcal{Q}_h yields the following inf-sup condition [42].

$$\sup_{\mathbf{v}_h \in \mathcal{V}_h} \frac{b(\mathbf{v}_h, q_h)}{\|\mathbf{v}_h\|_h} \geq \beta_1 \|q_h\|_{0, \Omega}, \tag{4.2}$$

where $\beta_1 > 0$ is independent of h . Hence, using (3.13) and the Babuška-Brezzi theory for saddle point problems we can assert that, for a given ϕ_h , there exists a unique solution to (3.9), (3.10). In particular, the existence of \mathbf{u}_h implies that of \mathbf{u}_h^N . To prove the existence and uniqueness of ϕ_h (and also in view of the error analysis to be presented later on), it is convenient to recast (3.8) employing the definition of $\mathcal{A}_h(\cdot, \cdot; \cdot, \cdot)$ in the following manner:

Find $\phi_h \in \mathcal{S}_h$ such that

$$\begin{aligned} \langle \partial_t \phi_h, \mathcal{R}^\sharp \varphi_h \rangle + B_h(\phi_h, \varphi_h; \chi_h) &= - \sum_{K \in \mathcal{T}_h} \sum_{j=1}^{d+1} \int_{s_{j+1} b_K s_j} \mathbf{u}_h^N \cdot \mathbf{n} \phi_h \mathcal{R}^\sharp \varphi_h \, ds \\ &\quad - \sum_{\sigma \in \mathcal{E}_h} \int_{\sigma} \{ \mathbf{u}_h^N \cdot \mathbf{n} \phi_h \}_\sigma \cdot \llbracket \mathcal{R}^\sharp \varphi_h \rrbracket_\sigma \, ds + l_h(\phi_h; \varphi_h) \quad \forall \varphi_h \in \mathcal{S}_h, \end{aligned} \quad (4.3)$$

where

$$\begin{aligned} B_h(\psi_h, \varphi_h; \chi_h) &:= - \sum_{K \in \mathcal{T}_h} \sum_{j=1}^{d+1} \int_{s_{j+1} b_K s_j} (\kappa(\chi_h) \nabla \psi_h) \cdot \mathbf{n} \mathcal{R}^\sharp \varphi_h \, ds + \sum_{\sigma \in \mathcal{E}_h} \int_{\sigma} \frac{\alpha_c}{h_\sigma} \llbracket \psi_h \rrbracket_\sigma \cdot \llbracket \varphi_h \rrbracket_\sigma \, ds \\ &\quad - \sum_{\sigma \in \mathcal{E}_h} \int_{\sigma} \{ (\kappa(\chi_h) \nabla \psi_h) \cdot \mathbf{n} \}_\sigma \cdot \llbracket \mathcal{R}^\sharp \varphi_h \rrbracket_\sigma \, ds - \sum_{\sigma \in \mathcal{E}_h} \int_{\sigma} \{ \kappa(\chi_h) (\nabla \varphi_h \cdot \mathbf{n}) \}_\sigma \cdot \llbracket \mathcal{R}^\sharp \psi_h \rrbracket_\sigma \, ds. \end{aligned}$$

Now, following the analysis presented in [11], we may prove the following result, valid within the ball $B_M = \{ \psi_h \in \mathcal{S}_h : \|\nabla \psi_h\|_\infty \leq M \}$.

Lemma 4.1. *The quantity*

$$E(\psi_h, \varphi_h; \chi_h) := - \sum_{K \in \mathcal{T}_h} \sum_{j=1}^{d+1} \int_{s_{j+1} b_K s_j} (\kappa(\chi_h) \nabla \psi_h) \cdot \mathbf{n} \mathcal{R}^\sharp \varphi_h \, ds - A(\psi_h, \varphi_h; \chi_h),$$

satisfies the estimate

$$|E(\psi_h, \varphi_h; \chi_h)| \leq Ch \|\psi_h\|_h \|\varphi_h\|_h \quad \forall \varphi_h, \psi_h \in \mathcal{S}_h, \chi_h \in B_M.$$

PROOF. Combining the definition of E and relation (3.11) we deduce that

$$\begin{aligned} E(\psi_h, \varphi_h; \chi_h) &= \sum_{K \in \mathcal{T}_h} \int_{\partial K} (\kappa(\chi_h) \nabla \psi_h) \cdot \mathbf{n} (\mathcal{R}^\sharp \varphi_h - \varphi_h) \, ds \\ &\quad + \sum_{K \in \mathcal{T}_h} \int_K \nabla \cdot (\kappa(\chi_h) \nabla \psi_h) (\varphi_h - \mathcal{R}^\sharp \varphi_h) \, dx =: T_1 + T_2. \end{aligned} \quad (4.4)$$

An application of (3.5), (2.3) and the fact that ψ_h and χ_h are linear on each triangle yields

$$\begin{aligned} \left| \int_{\partial K} \kappa(\chi_h) \nabla \psi_h \cdot \mathbf{n} (\varphi_h - \mathcal{R}^\sharp \varphi_h) \, ds \right| &\leq Ch \|\nabla(\kappa(\chi_h) \nabla \psi_h)\|_{0,K} \|\nabla \varphi_h\|_{0,K} \\ &\leq C\gamma_3 h \|\nabla \chi_h \cdot \nabla \psi_h\|_{0,K} \|\nabla \varphi_h\|_{0,K}. \end{aligned}$$

Using Hölder inequality, the fact that $\chi_h \in B_M$, and summation over all triangles, implies that

$$|T_1| \leq Ch \|\psi_h\|_h \|\varphi_h\|_h. \quad (4.5)$$

For T_2 , first we note that

$$\int_K \nabla \cdot (\kappa(\chi_h) \nabla \psi_h) (\varphi_h - \mathcal{R}^\sharp \varphi_h) \, dx \leq \|\nabla \cdot (\kappa(\chi_h) \nabla \psi_h)\|_{0,K} \|\varphi_h - \mathcal{R}^\sharp \varphi_h\|_{0,K}.$$

Now, by using (3.2), (2.3) and the fact ψ_h is linear on each K , we obtain

$$|T_2| \leq Ch \|\psi_h\|_h \|\varphi_h\|_h. \quad (4.6)$$

Combining the estimates obtained in (4.5) and (4.6) and inserting them in (4.4), we complete the proof.

Now, using Lemma 4.1 and following the proofs of Lemmas 2.3 and 2.4 in [22], we conclude that there exist generic positive constants β and C independent of h , but which may depend on the penalty parameter α_c , such that

$$\begin{aligned} B_h(\chi_h, \chi_h; \chi_h) &\geq \beta \|\chi_h\|_h^2 \quad \forall \chi_h \in B_M, \\ |B_h(\psi_h, \varphi_h; \chi_h)| &\leq C \|\psi_h\|_h \|\varphi_h\|_h \quad \forall \psi_h, \varphi_h \in \mathcal{S}_h \quad \forall \chi_h \in B_M. \end{aligned} \quad (4.7)$$

Using the trace inequality (3.6) and properties of \mathcal{R}^\sharp , for $\mathbf{u}(t) \in L^\infty(\Omega)$, the following bound has been derived in [20, p. 1364]:

$$\sum_{K \in \mathcal{T}_h} \sum_{j=1}^{d+1} \int_{s_{j+1} b_K s_j} \mathbf{u} \cdot \mathbf{n} \psi_h \mathcal{R}^\sharp \varphi_h \, ds \leq C \|\varphi_h\|_h (\|\psi_h\|_{0,\Omega} + h \|\psi_h\|_h) \quad \forall \psi_h \in \mathcal{S}(h), \forall \varphi_h \in \mathcal{S}_h. \quad (4.8)$$

Since \mathbf{u}_h^N is also uniformly bounded, (4.8) also holds true for \mathbf{u}_h^N . An application of the Cauchy-Schwarz inequality and the trace inequality together with the fact that \mathbf{u}_h^N is uniformly bounded yields

$$\int_\sigma \{\mathbf{u}_h^N \cdot \mathbf{n} \psi_h\}_\sigma \cdot \llbracket \mathcal{R}^\sharp \varphi_h \rrbracket_\sigma \, ds \leq C h_\sigma^{1/2} \left(h_K^{-1/2} \|\psi_h\|_{0,K} + h_K^{1/2} \|\nabla \psi_h\|_{0,K} \right) \frac{1}{h_\sigma^{1/2}} \|\llbracket \mathcal{R}^\sharp \varphi_h \rrbracket_\sigma\|_{0,\sigma}$$

Now, again using the Cauchy-Schwarz inequality together with definitions of \mathcal{R}^\sharp gives us

$$\begin{aligned} \frac{1}{h_\sigma^{1/2}} \|\llbracket \mathcal{R}^\sharp \varphi_h \rrbracket_\sigma\|_{0,\sigma} &= \frac{1}{h_\sigma^{1/2}} \left(\int_\sigma \llbracket \mathcal{R}^\sharp \varphi_h \rrbracket_\sigma^2 \, ds \right)^{1/2} = \llbracket \mathcal{R}^\sharp \varphi_h \rrbracket_\sigma = \frac{1}{h_\sigma} \int_\sigma \llbracket \varphi_h \rrbracket_\sigma \, ds \\ &\leq \frac{1}{h_\sigma} \left(\int_\sigma \llbracket \varphi_h \rrbracket_\sigma^2 \, ds \right)^{1/2} \left(\int_\sigma \, ds \right)^{1/2} = \left(\frac{1}{h_\sigma} \int_\sigma \llbracket \varphi_h \rrbracket_\sigma^2 \, ds \right)^{1/2}. \end{aligned} \quad (4.9)$$

Hence,

$$\int_\sigma \{\mathbf{u}_h^N \cdot \mathbf{n} \psi_h\}_\sigma \cdot \llbracket \mathcal{R}^\sharp \varphi_h \rrbracket_\sigma \, ds \leq C (\|\psi_h\|_{0,K} + h_K \|\nabla(\phi - \phi_h)\|_{0,K}) \left(\frac{1}{h_\sigma} \int_\sigma \llbracket \varphi_h \rrbracket_\sigma^2 \, ds \right)^{1/2}.$$

Summing over all edges and using the definition of the norm $\|\cdot\|_h$, we have for all $\psi_h, \varphi_h \in \mathcal{S}_h$

$$\sum_{\sigma \in \mathcal{E}_h} \int_\sigma \{\mathbf{u}_h^N \cdot \mathbf{n} \psi_h\}_\sigma \cdot \llbracket \mathcal{R}^\sharp \varphi_h \rrbracket_\sigma \, ds \leq C (\|\psi_h\|_{0,\Omega} + h \|\psi_h\|_h) \|\varphi_h\|_h. \quad (4.10)$$

In a similar way, using the Cauchy-Schwarz inequality and the trace inequality (3.6) and the same arguments used in (4.8) and (4.10), we obtain the following estimate

$$|l_h(\psi_h; \varphi_h)| \leq C (\|\psi_h\|_{0,\Omega} + h \|\psi_h\|_h) \|\varphi_h\|_h \quad \forall \psi_h \in \mathcal{S}(h), \forall \varphi_h \in \mathcal{S}_h. \quad (4.11)$$

Now, existence and uniqueness of ϕ_h can be shown as follows. Substituting \mathbf{u}_h^N in (4.3) gives a system of nonlinear differential equations in ϕ_h . An appeal to Picard's theorem guarantees the existence and uniqueness of ϕ_h in some small interval $(0, t_h)$ and in order to continue the solution an *a priori* bound for ϕ_h is required, which can be derived easily by employing the inequalities (4.8), (4.10), (4.11) and (4.7); for more detail, see [20]. Therefore, existence and uniqueness of ϕ_h is assured in a ball B_M .

4.2. Error estimates for velocity and pressure

For a given ϕ , we define the projection operators $(\tilde{\mathbf{u}}_h, \tilde{p}_h) : (0, T) \rightarrow \mathbf{V}_h \times \mathcal{Q}_h$ as follows:

$$\hat{A}_h(\tilde{\mathbf{u}}_h, \mathbf{v}_h; \phi) + c_h(\mathbf{v}_h, \tilde{p}_h) = d(\phi, \mathcal{P}^\sharp \mathbf{v}_h) \quad \forall \mathbf{v}_h \in \mathbf{V}_h, \quad (4.12)$$

$$b_h(\tilde{\mathbf{u}}_h, q_h) = 0 \quad \forall q_h \in \mathcal{Q}_h. \quad (4.13)$$

Now, the following estimates for $(\tilde{\mathbf{u}}_h, \tilde{p}_h) \in \mathbf{V}_h \times \mathcal{Q}_h$ can be derived by imitating the analysis of [13] (see also [42]):

$$\|\mathbf{u} - \tilde{\mathbf{u}}_h\|_{0,\Omega} \leq Ch^2(\|\mathbf{u}\|_{2,\Omega} + \|p\|_{1,\Omega} + \|\phi g\|_{1,\Omega}), \quad (4.14)$$

$$\|\mathbf{u} - \tilde{\mathbf{u}}_h\|_h + \|p - \tilde{p}_h\|_{0,\Omega} \leq Ch(\|\mathbf{u}\|_{2,\Omega} + \|p\|_{1,\Omega}). \quad (4.15)$$

Now in the following lemma, we discuss the error estimates for velocity and pressure in terms of concentration.

Lemma 4.3. *There exists a constant C independent of h , but which may depend on the bound of $\tilde{\mathbf{u}}_h$, such that*

$$\begin{aligned} \|\mathbf{u} - \mathbf{u}_h\|_{0,\Omega} &\leq Ch^2(\|\mathbf{u}\|_{2,\Omega} + \|p\|_{1,\Omega} + \|\phi g\|_{1,\Omega} + \|\phi - \phi_h\|_{0,\Omega} + h\|\phi - \phi_h\|_h), \\ \|\mathbf{u} - \mathbf{u}_h\|_h + \|p - \tilde{p}_h\|_{0,\Omega} &\leq Ch(\|\mathbf{u}\|_{2,\Omega} + \|p\|_{1,\Omega} + \|\phi - \phi_h\|_{0,\Omega} + h\|\phi - \phi_h\|_h). \end{aligned}$$

PROOF. Write $\mathbf{u} - \mathbf{u}_h = \mathbf{u} - \tilde{\mathbf{u}}_h + \tilde{\mathbf{u}}_h - \mathbf{u}_h$ and $p - p_h = p - \tilde{p}_h + \tilde{p}_h - p_h$. Since estimates for $\mathbf{u} - \tilde{\mathbf{u}}_h$ and $p - \tilde{p}_h$ are given in (4.14) and (4.15), we proceed to find estimates for $\tilde{\mathbf{u}}_h - \mathbf{u}_h$ and $\tilde{p}_h - p_h$. Subtracting (3.9) from (4.12) and (3.10) from (4.13), respectively, we get for all $\mathbf{v}_h \in \mathbf{V}_h$ and $q_h \in \mathcal{Q}_h$

$$\hat{A}_h(\tilde{\mathbf{u}}_h, \mathbf{v}_h; \phi) - \hat{A}_h(\mathbf{u}_h, \mathbf{v}_h; \phi_h) + c_h(\mathbf{v}_h, \tilde{p}_h) - c_h(\mathbf{v}_h, p_h) = d(\phi, \mathcal{P}^\sharp \mathbf{v}_h) - d(\phi_h, \mathcal{P}^\sharp \mathbf{v}_h), \quad (4.16)$$

$$b_h(\tilde{\mathbf{u}}_h - \mathbf{u}_h, q_h) = 0. \quad (4.17)$$

We rewrite (4.16) as follows:

$$\begin{aligned} \hat{A}_h(\tilde{\mathbf{u}}_h - \mathbf{u}_h, \mathbf{v}_h; \phi_h) + c_h(\mathbf{v}_h, \tilde{p}_h - p_h) &= \hat{A}_h(\tilde{\mathbf{u}}_h, \mathbf{v}_h; \phi_h) - \hat{A}_h(\mathbf{u}_h, \mathbf{v}_h; \phi) \\ &\quad + d(\phi, \mathcal{P}^\sharp \mathbf{v}_h) - d(\phi_h, \mathcal{P}^\sharp \mathbf{v}_h) \quad \forall \mathbf{v}_h \in \mathbf{V}_h. \end{aligned}$$

By using the definition of $\hat{A}_h(\cdot, \cdot; \cdot)$, (3.12) and the fact that $\tilde{\mathbf{u}}_h$ is linear on K , we can write

$$\begin{aligned} \hat{A}_h(\tilde{\mathbf{u}}_h, \mathbf{v}_h; \phi_h) - \hat{A}_h(\mathbf{u}_h, \mathbf{v}_h; \phi) &= [\hat{A}(\tilde{\mathbf{u}}_h, \mathbf{v}_h; \phi_h) - \hat{A}(\tilde{\mathbf{u}}_h, \mathbf{v}_h; \phi)] \\ &\quad + \sum_{K \in \mathcal{T}_h} \int_{\partial K} (\mu(\phi_h) - \mu(\phi)) (\mathcal{P}^\sharp \mathbf{v}_h - \mathbf{v}_h) \boldsymbol{\varepsilon}(\tilde{\mathbf{u}}_h) \cdot \mathbf{n} \, ds \\ &\quad + \sum_{\sigma \in \mathcal{E}_h} \int_{\sigma} \{(\mu(\phi_h) - \mu(\phi)) \boldsymbol{\varepsilon}(\tilde{\mathbf{u}}_h) \mathbf{n}\}_{\sigma} \cdot \llbracket \mathcal{P}^\sharp \mathbf{v}_h \rrbracket_{\sigma} \, ds \\ &\quad + \sum_{\sigma \in \mathcal{E}_h} \int_{\sigma} \{(\mu(\phi_h) - \mu(\phi)) \boldsymbol{\varepsilon}(\mathbf{v}_h) \mathbf{n}\}_{\sigma} \cdot \llbracket \mathcal{P}^\sharp \tilde{\mathbf{u}}_h \rrbracket_{\sigma} \, ds \\ &\quad + \sum_{K \in \mathcal{T}_h} \int_K (\nabla \cdot \mu(\phi_h) - \nabla \cdot \mu(\phi)) \boldsymbol{\varepsilon}(\tilde{\mathbf{u}}_h) \cdot (\mathbf{v}_h - \mathcal{P}^\sharp \mathbf{v}_h) \, dx \\ &=: J_1 + J_2 + J_3 + J_4 + J_5. \end{aligned} \quad (4.18)$$

Since the mesh \mathcal{T}_h is quasi-uniform, we assume that there exist constant C independent of h such that

$$\|\nabla \cdot \tilde{\mathbf{u}}_h\|_{\infty, K} + \|\nabla \cdot \tilde{\mathbf{u}}_h\|_{\infty, \partial K} \leq C \quad \forall K \in \mathcal{T}_h. \quad (4.19)$$

Employing the definition of $\hat{A}(\cdot, \cdot; \cdot)$, (4.19), the Lipschitz continuity of μ and the Cauchy-Schwarz inequality, we have the following bound for J_1 .

$$|J_1| \leq C \|\phi - \phi_h\|_{0,\Omega} \|\mathbf{v}_h\|_h.$$

In order to bound J_2 , first we note that by using Cauchy-Schwarz inequality, (4.19), trace inequality (3.6) and (3.3)

$$\begin{aligned} & \left| \int_{\partial K} (\mu(\phi_h) - \mu(\phi)) (\mathcal{P}^\sharp \mathbf{v}_h - \mathbf{v}_h) \boldsymbol{\varepsilon}(\tilde{\mathbf{u}}_h) : \mathbf{n} \, ds \right| \\ & \leq C \left(h_K^{-1/2} \|\phi - \phi_h\|_{0,K} + h_K^{1/2} \|\nabla(\phi - \phi_h)\|_{0,K} \right) h_K^{-1/2} \|\mathcal{P}^\sharp \mathbf{v}_h - \mathbf{v}_h\|_{0,K} \\ & \leq C (\|\phi - \phi_h\|_{0,K} + h_K \|\nabla(\phi - \phi_h)\|_{0,K}) \|\nabla \cdot \mathbf{v}_h\|_{0,K}. \end{aligned}$$

Now summing over all triangles and using definitions of the mesh dependent norms $\|\cdot\|_h$ and $\|\!\|\!\cdot\!\|\!$, we have

$$|J_2| \leq C (\|\phi - \phi_h\|_{0,\Omega} + h \|\!\|\phi - \phi_h\!\!\|_h) \|\mathbf{v}_h\|_h.$$

Similarly, to bound J_3 again an application of Cauchy-Schwarz inequality, (4.19) and trace inequality (3.6) yields

$$\begin{aligned} & \left| \int_{\sigma} \{(\mu(\phi_h) - \mu(\phi)) \boldsymbol{\varepsilon}(\tilde{\mathbf{u}}_h) \mathbf{n}\}_{\sigma} \cdot \llbracket \mathcal{P}^\sharp \mathbf{v}_h \rrbracket_{\sigma} \, ds \right| \\ & \leq C h_{\sigma}^{1/2} \left(h_K^{-1/2} \|\phi - \phi_h\|_{0,K} + h_K^{1/2} \|\nabla(\phi - \phi_h)\|_{0,K} \right) \frac{1}{h_{\sigma}^{1/2}} \|\llbracket \mathcal{P}^\sharp \mathbf{v}_h \rrbracket_{\sigma}\|_{0,\sigma}. \end{aligned}$$

Using (4.9), we obtain

$$\begin{aligned} & \left| \int_{\sigma} \{(\mu(\phi_h) - \mu(\phi)) \boldsymbol{\varepsilon}(\tilde{\mathbf{u}}_h) \mathbf{n}\}_{\sigma} \cdot \llbracket \mathcal{P}^\sharp \mathbf{v}_h \rrbracket_{\sigma} \, ds \right| \\ & \leq C (\|\phi - \phi_h\|_{0,K} + h \|\nabla(\phi - \phi_h)\|_{0,K}) \left(\frac{1}{h_{\sigma}} \int_{\sigma} \llbracket \mathbf{v}_h \rrbracket_{\sigma}^2 \, ds \right)^{1/2}. \end{aligned}$$

Now summing over all the edges and using definitions of $\|\cdot\|_h$ and $\|\!\|\!\cdot\!\!\|_h$, we have

$$|J_3| \leq C (\|\phi - \phi_h\|_{0,\Omega} + h \|\!\|\phi - \phi_h\!\!\|_h) \|\mathbf{v}_h\|_h. \quad (4.20)$$

To bound J_4 , note that (3.4) implies $\llbracket \mathcal{P}^\sharp \tilde{\mathbf{u}}_h \rrbracket_{\sigma} = \llbracket \mathcal{P}^\sharp (\tilde{\mathbf{u}}_h - \mathbf{u}) \rrbracket_{\sigma}$. Now, a repeated application of the trace inequality (3.6) and the inverse inequality $\|\psi_h\|_{\infty, \partial K} \leq C h_K^{-1} \|\psi\|_{0, \partial K}$ together with fact that \mathbf{v}_h is linear and $\mathcal{P}^\sharp(\cdot)$ is constant on triangle K yields

$$\begin{aligned} & \int_{\sigma} \{(\mu(\phi_h) - \mu(\phi)) \boldsymbol{\varepsilon}(\mathbf{v}_h) \mathbf{n}\}_{\sigma} \cdot \llbracket \mathcal{P}^\sharp \tilde{\mathbf{u}}_h \rrbracket_{\sigma} \, ds \leq \|\boldsymbol{\varepsilon}(\mathbf{v}_h)\|_{\infty, \sigma} \|\phi - \phi_h\|_{0, \sigma} \|\llbracket \mathcal{P}^\sharp (\tilde{\mathbf{u}}_h - \mathbf{u}) \rrbracket_{\sigma}\|_{0, \sigma} \\ & \leq C h_K^{-1} \|\boldsymbol{\varepsilon}(\mathbf{v}_h)\|_{0, \sigma} \left(h_K^{-1/2} \|\phi - \phi_h\|_{0, K} + h_K^{1/2} \|\nabla(\phi - \phi_h)\|_{0, K} \right) h_K^{-1/2} \|\mathcal{P}^\sharp (\tilde{\mathbf{u}}_h - \mathbf{u})\|_{0, K} \\ & \leq C h_K^{-2} \|\boldsymbol{\varepsilon}(\mathbf{v}_h)\|_{0, K} (\|\phi - \phi_h\|_{0, K} + h_K \|\nabla(\phi - \phi_h)\|_{0, K}) \|\mathcal{P}^\sharp (\tilde{\mathbf{u}}_h - \mathbf{u})\|_{0, K}. \end{aligned}$$

Now, using the L^2 -stability of \mathcal{P}^\sharp , i.e., $\|\mathcal{P}^\sharp \mathbf{v}_h\|_{0, \Omega} \leq C \|\mathbf{v}_h\|_{0, \Omega}$ for all $\mathbf{v}_h \in \mathbf{V}_h$ and (4.14), we have

$$\int_{\sigma} \{(\mu(\phi_h) - \mu(\phi)) \boldsymbol{\varepsilon}(\mathbf{v}_h) \mathbf{n}\}_{\sigma} \cdot \llbracket \mathcal{P}^\sharp \tilde{\mathbf{u}}_h \rrbracket_{\sigma} \, ds \leq C \|\boldsymbol{\varepsilon}(\mathbf{v}_h)\|_{0, K} (\|\phi - \phi_h\|_{0, K} + h_K \|\nabla(\phi - \phi_h)\|_{0, K}),$$

and summing over all edges we get

$$|J_4| \leq C (\|\phi - \phi_h\|_{0,\Omega} + h \|\!\|\phi - \phi_h\!\!\|_h) \|\mathbf{v}_h\|_h. \quad (4.21)$$

For J_5 , first we note that

$$\nabla \cdot \mu(\phi_h) - \nabla \cdot \mu(\phi) = \mu'(\phi_h) (\nabla \phi_h - \nabla \phi) + \nabla \phi (\mu'(\phi_h) - \mu'(\phi)).$$

Now using Lipschitz continuity and boundedness of μ' and similar arguments used in the bound for J_1 , the following bound for J_5 can be obtained easily:

$$|J_5| \leq Ch(\|\phi - \phi_h\|_{0,\Omega} + \|\phi - \phi_h\|_h) \|\mathbf{v}_h\|_h.$$

Putting together all derived bounds for J_1, \dots, J_5 in (4.18), we have

$$|\hat{A}_h(\tilde{\mathbf{u}}_h, \mathbf{v}_h; \phi_h) - \hat{A}_h(\tilde{\mathbf{u}}_h, \mathbf{v}_h; \phi)| \leq C(\|\phi - \phi_h\|_{0,\Omega} + h\|\phi - \phi_h\|_h) \|\mathbf{v}_h\|_h. \quad (4.22)$$

In view of the definition of $d(\cdot, \mathcal{P}^\sharp)$ and the fact that $\|\mathcal{P}^\sharp \mathbf{v}_h\|_{0,\Omega} \leq C\|\mathbf{v}_h\|_{0,\Omega} \leq C\|\mathbf{v}_h\|_h$ for all $\mathbf{v}_h \in \mathcal{V}_h$, it is easy to see that

$$|d(\phi, \mathcal{P}^\sharp \mathbf{v}_h) - d(\phi_h, \mathcal{P}^\sharp \mathbf{v}_h)| \leq C\|\phi - \phi_h\|_{0,\Omega} \|\mathbf{v}_h\|_h. \quad (4.23)$$

Now, choosing $\mathbf{v}_h = \tilde{\mathbf{u}}_h - \mathbf{u}_h$ and using (3.13), (4.17), and the coercivity of \hat{A}_h together with (4.22) and (4.23), we obtain the following bound for $\tilde{\mathbf{u}}_h - \mathbf{u}_h$:

$$\|\tilde{\mathbf{u}}_h - \mathbf{u}_h\|_h \leq C(\|\phi - \phi_h\|_{0,\Omega} + h\|\phi - \phi_h\|_h). \quad (4.24)$$

In order to find a bound for $\tilde{p}_h - p_h$, we again choose $\mathbf{v}_h = \tilde{\mathbf{u}}_h - \mathbf{u}_h$ and employ (4.22), (4.23) and (3.13) to obtain

$$|B(\tilde{\mathbf{u}}_h - \mathbf{u}_h, \tilde{p}_h - p_h)| \leq C(\|\phi - \phi_h\|_{0,\Omega} + h\|\phi - \phi_h\|_h + \|\tilde{\mathbf{u}}_h - \mathbf{u}_h\|_h) \|\tilde{\mathbf{u}}_h - \mathbf{u}_h\|_h.$$

By an application of the inf-sup condition given in (4.2) and using (4.24), we arrive at

$$\|\tilde{p}_h - p_h\|_{0,\Omega} \leq C(\|\phi - \phi_h\|_{0,\Omega} + h\|\phi - \phi_h\|_h).$$

The L^2 -norm estimate of $\tilde{\mathbf{u}}_h - \mathbf{u}_h$ follows from $\|\mathbf{v}_h\|_{0,\Omega} \leq C\|\mathbf{v}_h\|_h$ for all $\mathbf{v}_h \in \mathcal{V}_h$, and after employing (4.14) and (4.15), we obtain the desired result.

4.3. Error estimates for the concentration field

We decompose the error in $\phi - \phi_h$ as

$$\phi - \phi_h = \eta + \theta, \quad \eta := \phi - R_h\phi, \quad \theta := R_h\phi - \phi_h, \quad (4.25)$$

where $R_h : H^1(\Omega) \rightarrow \mathcal{S}_h$ is the elliptic projection defined as

$$B_h(\phi - R_h\phi, \varphi_h; \phi) = 0 \quad \forall \varphi_h \in \mathcal{S}_h. \quad (4.26)$$

Lemma 4.5. *There exists a positive constant C independent of h such that*

$$\|\phi - R_h\phi\|_h \leq Ch\|\phi\|_{2,\Omega}, \quad (4.27)$$

$$\|\phi - R_h\phi\|_{0,\Omega} \leq C(\phi, \mathbf{f}, \mathbf{u}) h^2. \quad (4.28)$$

PROOF. Let us write $\phi - R_h\phi = \phi - I_h\phi + I_h\phi - R_h\phi$, where $I_h\phi$ denotes the interpolant of ϕ which satisfies the following approximation properties:

$$|\phi - I_h\phi|_{s,K} \leq Ch_K^{2-s} \|\phi\|_{2,K} \quad \forall K \in \mathcal{T}_h \text{ and } s = 0, 1. \quad (4.29)$$

Using the definition of $\|\cdot\|$, it is easy to see that for a given ϕ , $B_h(\cdot, \cdot; \phi)$ is bounded in the following sense (see Lemma 2.4 in [22]):

$$|B_h(\psi, \varphi; \phi)| \leq \|\psi\| \|\varphi\| \quad \forall \psi, \varphi \in \mathcal{S}(h). \quad (4.30)$$

From the definition of $\|\cdot\|$ and (4.29), we obtain

$$\|\phi - I_h\phi\| \leq Ch\|\phi\|_{2,\Omega}.$$

Now using (4.30) and (4.7) together with the definition of R_h , we have

$$\begin{aligned} \beta \|I_h\phi - R_h\phi\|_h^2 &\leq B_h(I_h\phi - R_h\phi, I_h\phi - R_h\phi; \phi) = B_h(I_h\phi - \phi, I_h\phi - R_h\phi; \phi) \\ &\leq C \|\phi - I_h\phi\| \|I_h\phi - R_h\phi\|_h, \end{aligned}$$

and hence,

$$\|I_h\phi - R_h\phi\|_h \leq C \|\phi - I_h\phi\|. \quad (4.31)$$

Now, (4.27) follows after using (4.29) and (4.31). For deriving the L^2 - norm estimates, we first define the following form:

$$\begin{aligned} A_1(\psi_h, \varphi_h; \chi_h) &:= A(\psi_h, \varphi_h; \chi_h) - \sum_{\sigma \in \mathcal{E}_h} \int_{\sigma} \{(\kappa(\chi_h)\nabla\psi_h) \cdot \mathbf{n}\}_{\sigma} \cdot \llbracket \varphi_h \rrbracket_{\sigma} \, ds \\ &\quad - \sum_{\sigma \in \mathcal{E}_h} \int_{\sigma} \{\kappa(\chi_h)(\nabla\varphi_h \cdot \mathbf{n})\}_{\sigma} \cdot \llbracket \psi_h \rrbracket_{\sigma} \, ds + \sum_{\sigma \in \mathcal{E}_h} \int_{\sigma} \frac{\alpha_c}{h_{\sigma}} \llbracket \psi_h \rrbracket_{\sigma} \cdot \llbracket \varphi_h \rrbracket_{\sigma} \, ds. \end{aligned}$$

Then first we find the error between $B_h(\cdot, \cdot; \phi)$ and $A_1(\cdot, \cdot; \phi)$. The error on elements (K) as well as on the boundary integrals (∂K) can be computed by following the analysis of [11] and error on the edges (σ) by using the same arguments used in Lemma 3.1 of [22]. Then standard duality arguments can be used to derived optimal error estimates in $\|\phi - R_h\phi\|_{0,\Omega}$ given in (4.28). For detailed proof, we refer to Theorem 4.4 in [11], Lemma 4.4 in [20] and also see [22].

The quasi-uniformity of the mesh implies that there exists a constant C independent of h such that (see Theorem 4.7 in [3] and also [30])

$$\|\nabla R_h\phi\|_{\infty,K} \leq C, \quad \|\nabla R_h\phi\|_{\infty,\partial K} \leq C, \quad \|R_h\phi\|_{\infty,K} \leq C, \quad \|R_h\phi\|_{\infty,\partial K} \leq C. \quad (4.32)$$

Now we provide appropriate estimates for θ (see (4.25)).

Lemma 4.7. *There exists a constant C independent of h such that*

$$\begin{aligned} &\|\theta\|_{0,\Omega}^2 + \beta_* \int_0^T \|\theta\|_h^2 \, d\tau \\ &\leq C \int_0^t \left(h^4 (\|\mathbf{u}\|_{2,\Omega}^2 + \|p\|_{1,\Omega}^2 + \|\phi g\|_{1,\Omega}^2) + h^2 \|\eta\|_h^2 + \|\eta\|_{0,\Omega}^2 + \|\partial_t \eta\|_{0,\Omega}^2 \right) d\tau. \end{aligned}$$

PROOF. First we note that ϕ and $\mathbf{u} = \mathbf{u}^N$ (where we take N large enough in the definition of \mathcal{N} such that $|\mathbf{u}(x)| \leq N$) satisfy

$$\begin{aligned} \langle \partial_t \phi, \mathcal{R}^{\sharp} \varphi_h \rangle + B_h(\phi, \varphi_h; \phi) &= - \sum_{K \in \mathcal{T}_h} \sum_{j=1}^{d+1} \int_{s_{j+1} b_K s_j} \mathbf{u}^N \cdot \mathbf{n} \phi \mathcal{R}^{\sharp} \varphi_h \, ds \\ &\quad - \sum_{\sigma \in \mathcal{E}_h} \int_{\sigma} \{\mathbf{u}^N \cdot \mathbf{n} \phi\}_{\sigma} \cdot \llbracket \mathcal{R}^{\sharp} \varphi_h \rrbracket_{\sigma} \, ds + l_h(\phi; \varphi_h) \quad \forall \varphi_h \in \mathcal{S}_h. \end{aligned} \quad (4.33)$$

Subtracting (4.3) from (4.33), we obtain the following error equation in terms of η and θ :

$$\begin{aligned}
\langle \partial_t \theta, \mathcal{R}^\sharp \varphi_h \rangle + B_h(\theta, \varphi_h; \phi_h) &= [-B_h(\phi, \varphi_h; \phi) - B_h(\eta, \varphi_h; \phi_h) + B_h(\phi, \varphi_h; \phi_h)] \\
&+ \sum_{K \in \mathcal{T}_h} \sum_{j=1}^{d+1} \int_{s_{j+1} b_K s_j} (\mathbf{u}_h^N - \mathbf{u}^N) \cdot \mathbf{n} \phi \mathcal{R}^\sharp \varphi_h \, ds \\
&+ \sum_{K \in \mathcal{T}_h} \sum_{j=1}^{d+1} \int_{s_{j+1} b_K s_j} (\phi_h - \phi) \mathbf{u}_h^N \cdot \mathbf{n} \mathcal{R}^\sharp \varphi_h \, ds \\
&+ \sum_{\sigma \in \mathcal{E}_h} \int_{\sigma} \{(\mathbf{u}_h^N - \mathbf{u}^N) \cdot \mathbf{n}\}_{\sigma} \cdot \llbracket \mathcal{R}^\sharp \varphi_h \rrbracket_{\sigma} \, ds \\
&+ \sum_{\sigma \in \mathcal{E}_h} \int_{\sigma} \{(\phi_h - \phi) \mathbf{n} \cdot \mathbf{u}_h^N\}_{\sigma} \cdot \llbracket \mathcal{R}^\sharp \varphi_h \rrbracket_{\sigma} \, ds \\
&- \langle \partial_t \eta, \mathcal{R}^\sharp \varphi_h \rangle + l_h(\phi - \phi_h; \varphi_h) \\
&=: I_1 + I_2 + I_3 + I_4 + I_5 + I_6 + I_7.
\end{aligned} \tag{4.34}$$

Now we estimate I_1, \dots, I_7 one by one. By using (4.26), we have

$$B_h(\phi, \varphi_h; \phi_h) - B_h(\phi, \varphi_h; \phi) - B_h(\eta, \varphi_h; \phi_h) = B_h(R_h \phi, \varphi_h; \phi_h) - B_h(R_h \phi, \varphi_h; \phi),$$

and hence by using the definition of $B_h(\cdot, \cdot; \cdot)$, we have

$$\begin{aligned}
B_h(R_h \phi, \varphi_h; \phi_h) - B_h(R_h \phi, \varphi_h; \phi) &= \sum_{K \in \mathcal{T}_h} \sum_{j=1}^{d+1} \int_{s_{j+1} b_K s_j} (\kappa(\phi) - \kappa(\phi_h)) \nabla(R_h \phi) \cdot \mathbf{n} \mathcal{R}^\sharp \varphi_h \, ds \\
&+ \sum_{\sigma \in \mathcal{E}_h} \int_{\sigma} \{(\kappa(\phi) - \kappa(\phi_h)) \nabla(R_h \phi)\}_{\sigma} \cdot \llbracket \mathcal{R}^\sharp \varphi_h \rrbracket_{\sigma} \, ds \\
&+ \sum_{\sigma \in \mathcal{E}_h} \int_{\sigma} \{(\kappa(\phi) - \kappa(\phi_h)) \nabla \varphi_h \cdot \mathbf{n}\}_{\sigma} \cdot \llbracket \mathcal{R}^\sharp(R_h \phi) \rrbracket_{\sigma} \, ds \\
&=: T_1 + T_2 + T_3.
\end{aligned}$$

Using (3.11), we rewrite T_1 as

$$\begin{aligned}
T_1 &= [A(R_h \phi, \varphi_h; \phi_h) - A(R_h \phi, \varphi_h; \phi)] + \sum_{K \in \mathcal{T}_h} \int_{\partial K} (\kappa(\phi_h) - \kappa(\phi)) \nabla(R_h \phi) \cdot \mathbf{n} (\mathcal{R}^\sharp \varphi_h - \varphi_h) \, ds \\
&+ \sum_{K \in \mathcal{T}_h} \int_K \nabla[(\kappa(\phi_h) - \kappa(\phi)) \nabla(R_h \phi)] (\varphi_h - \mathcal{R}^\sharp \varphi_h) \, dx =: T_1^1 + T_1^2 + T_1^3.
\end{aligned}$$

Employing the definition of $A(\cdot, \cdot; \cdot)$ together with Cauchy-Schwarz inequality and (4.32), we obtain

$$|T_1^1| \leq C \|\phi - \phi_h\|_{0,\Omega} \|\phi_h\|_h.$$

Again, an application of (4.32) together with trace inequality (3.6) and (3.3) yields

$$\begin{aligned}
&\int_{\partial K} (\kappa(\phi_h) - \kappa(\phi)) \nabla(R_h \phi) \cdot \mathbf{n} (\mathcal{R}^\sharp \varphi_h - \varphi_h) \, ds \\
&\leq C \left(h_K^{-1/2} \|\phi - \phi_h\|_{0,K} + h_K^{1/2} \|\nabla(\phi - \phi_h)\|_{0,K} \right) \\
&\quad \times \left(h_K^{-1/2} \|\mathcal{R}^\sharp \varphi_h - \varphi_h\|_{0,K} + h_K^{1/2} \|\nabla(\mathcal{R}^\sharp \varphi_h - \varphi_h)\|_{0,K} \right) \\
&\leq C (\|\phi - \phi_h\|_{0,K} + h_K \|\nabla(\phi - \phi_h)\|_{0,K}) \|\nabla \varphi_h\|_{0,K}.
\end{aligned}$$

Then, summation over all triangles gives

$$|T_1^2| \leq C(\|\phi - \phi_h\|_{0,\Omega} + h\|\phi - \phi_h\|_h)\|\varphi_h\|_h.$$

To estimate T_1^3 , we argue as follows: Since $R_h\phi$ is linear on each triangle, we note that

$$\begin{aligned} \nabla \cdot [(\kappa(\phi_h) - \kappa(\phi))\nabla R_h\phi] &= (\nabla\kappa(\phi_h) - \nabla\kappa(\phi)) \cdot \nabla(R_h\phi) = (\kappa'(\phi_h)\nabla\phi_h - \kappa'(\phi)\nabla\phi) \cdot \nabla(R_h\phi) \\ &= [\kappa'(\phi_h)(\nabla\phi_h - \nabla\phi) + \nabla\phi(\kappa'(\phi_h) - \kappa'(\phi))] \cdot \nabla(R_h\phi), \end{aligned}$$

and therefore, by assuming that κ' is Lipschitz continuous and using Cauchy-Schwarz inequality, (3.3), (4.32), (2.3), we have

$$|T_1^3| \leq C(\gamma_3)h(\|\phi - \phi_h\|_{0,\Omega} + \|\phi - \phi_h\|_h)\|\varphi_h\|_h.$$

By putting together estimates of T_1^1, T_1^2 and T_1^3 , we obtain the following bound for T_1 :

$$|T_1| \leq C(\|\phi - \phi_h\|_{0,\Omega} + h\|\phi - \phi_h\|_h)\|\varphi_h\|_h.$$

For T_2 , we use the same arguments used in the bound for J_3 given in (4.20) and (4.32) to obtain

$$|T_2| \leq C(\|\phi - \phi_h\|_{0,\Omega} + h\|\phi - \phi_h\|_h)\|\varphi_h\|_h.$$

To bound T_3 , first we note that from (3.4), we have $\llbracket \mathcal{R}^\sharp R_h\phi \rrbracket_\sigma = \llbracket \mathcal{R}^\sharp(R_h\phi - \phi) \rrbracket_\sigma$. Now following the same techniques used in the bound of J_4 given in (4.21), where (4.28) is used in place of (4.14), we immediately conclude that

$$|T_3| \leq C(\|\phi - \phi_h\|_{0,\Omega} + h\|\phi - \phi_h\|_h)\|\varphi_h\|_h,$$

and hence,

$$|I_1| \leq C(\|\phi - \phi_h\|_{0,\Omega} + h\|\phi - \phi_h\|_h)\|\varphi_h\|_h.$$

Using (4.1) and the uniform boundedness of \mathbf{u}_h^N , we have from (4.8)

$$|I_2|, |I_3| \leq C(\|\mathbf{u} - \mathbf{u}_h\| + h\|\mathbf{u} - \mathbf{u}_h\|_h)\|\varphi_h\|_h.$$

Again using the same techniques which were used to bound J_3 together with (4.1) and $\mathbf{u}_h^N \in L^\infty(\Omega)$, we easily obtain the following bounds for I_4 and I_5

$$|I_4|, |I_5| \leq C(\|\mathbf{u} - \mathbf{u}_h\| + h\|\mathbf{u} - \mathbf{u}_h\|_h)\|\varphi_h\|_h.$$

An application of the Cauchy-Schwarz inequality together with L^2 stability of \mathcal{R}^\sharp , i.e., $\|\mathcal{R}^\sharp\varphi_h\| \leq C\|\varphi_h\|_{0,\Omega}$ for all $\varphi_h \in \mathcal{S}_h$ yields

$$|I_6| \leq C\|\partial_t\eta\|_{0,\Omega}\|\varphi_h\|_{0,\Omega}.$$

With the help of (4.11) and the assumption that \mathbf{f} is Lipschitz continuous, we have

$$|I_7| \leq C(\|\phi - \phi_h\| + h\|\phi - \phi_h\|_h)\|\varphi_h\|.$$

Choosing $\varphi_h = \theta$, substituting all the estimates of I_1, \dots, I_7 into (4.34) and using Lemma 4.3 together with (4.7) and Young's inequality ($ab \leq \frac{\xi}{2}a^2 + \frac{1}{2\xi}b^2$ for all $a, b \in \mathbb{R}$ and $\xi > 0$) and standard kick-back techniques, we arrive at

$$\begin{aligned} &\langle \partial_t\theta, \mathcal{R}^\sharp\theta \rangle + (\beta - \xi)\|\theta\|_h^2 \\ &\leq C\left(\|\theta\|_{0,\Omega}^2 + h^4(\|\mathbf{u}\|_{2,\Omega}^2 + \|p\|_{1,\Omega}^2 + \|\phi g\|_{1,\Omega}^2) + h^2\|\eta\|_h^2 + \|\eta\|_{0,\Omega}^2 + \|\partial_t\eta\|_{0,\Omega}^2\right). \end{aligned} \quad (4.35)$$

h	$e_0(\phi)$	rate	$e_h(\phi)$	rate	$e_0(\mathbf{u})$	rate	$e_h(\mathbf{u})$	rate	$e_0(p)$	rate
0.282843	0.000417	—	0.014682	—	0.005051	—	0.084452	—	0.090676	—
0.141421	9.985e-5	2.064360	0.007517	0.965799	0.001362	1.890035	0.043453	0.958673	0.045269	1.002196
0.070710	2.443e-5	2.031181	0.003793	0.986676	0.000352	1.949367	0.022022	0.980517	0.022593	1.002608
0.035355	6.124e-6	1.998820	0.001903	0.995063	8.971e-5	1.976015	0.011082	0.990626	0.011285	1.001441
0.017677	1.742e-6	1.996747	0.000951	1.000251	2.260e-5	1.988362	0.005559	0.995415	0.005640	1.000632
0.008838	4.385e-7	1.968233	0.000473	1.007512	5.676e-6	1.993964	0.002783	0.997734	0.002819	1.000232
0.004419	1.097e-7	1.957892	0.000235	1.009310	1.423e-6	1.995512	0.001393	0.998874	0.001409	1.000091
0.002207	2.562e-8	1.930530	0.000121	1.001002	3.671e-7	1.992075	0.000702	0.999513	0.000702	1.000002

Table 1: Example 1: Convergence test against an analytical solution employing DFVE approximations of concentration, velocity and pressure computed on a sequence of uniformly refined triangulations of the unit square.

Let us define the following norm:

$$\|\varphi_h\|_1 := (\varphi_h, \mathcal{R}^\sharp \varphi_h)$$

Using properties of \mathcal{R}^\sharp , it is easy to prove the following, see [20, pp. 1365]:

$$(\varphi_h, \mathcal{R}^\sharp \psi_h) = (\varphi_h, \mathcal{R}^\sharp \psi_h) \quad \forall \varphi_h, \psi_h \in \mathcal{S}_h. \quad (4.36)$$

Moreover, $\|\cdot\|_1$ and $\|\cdot\|_{0,\Omega}$ are equivalent, i.e., there exist $C_1 > 0$ and $C_2 > 0$ independent of h such that

$$C_1 \|\psi_h\|_{0,\Omega} \leq \|\psi_h\|_1 \leq C_2 \|\psi_h\|_{0,\Omega} \quad \forall \psi_h \in \mathcal{S}_h. \quad (4.37)$$

Employing (4.36), we obtain from (4.35)

$$\frac{1}{2} \frac{d}{dt} (\theta, \mathcal{R}^\sharp \theta) + \beta_* \|\theta\|_h^2 \leq C \left(\|\theta\|_{0,\Omega}^2 + \|\mathbf{u} - \mathbf{u}_h\|_{0,\Omega}^2 + h^2 \|\mathbf{u} - \mathbf{u}_h\|_h^2 + h^2 \|\eta\|_h^2 + \|\eta\|_{0,\Omega}^2 + \|\partial_t \eta\|_{0,\Omega}^2 \right).$$

We proceed to choose $\phi_h(0) = R_h \phi(0)$, which implies that $\theta(0) = 0$. Now, an application of Gronwall's inequality together with (4.37) enable us to write

$$\|\theta\|_{0,\Omega}^2 + \beta_* \int_0^T \|\theta\|_h^2 d\tau \leq C \int_0^T \left(h^4 (\|\mathbf{u}\|_{2,\Omega}^2 + \|p\|_{1,\Omega}^2 + \|\phi g\|_{1,\Omega}^2) + h^2 \|\eta\|_h^2 + \|\eta\|_{0,\Omega}^2 + \|\partial_t \eta\|_{0,\Omega}^2 \right) d\tau,$$

which completes the proof.

Theorem 4.9 (Error estimates). *Let $(\phi_h(t), \mathbf{u}_h(t), p_h(t)) \in \mathcal{S}_h \times \mathcal{V}_h \times \mathcal{Q}_h$ be the unique solution of (3.8)-(3.10) and $(\phi(t), \mathbf{u}(t), p(t))$ the unique solution of (2.5) for a fixed time $t < T$. Then, under the assumption that $\phi_h(0) = R_h \phi(0)$, there exists $C > 0$ such that*

$$\|\phi(t) - \phi_h(t)\|_{0,\Omega} \leq C(\phi, \phi_t, \mathbf{f}, \mathbf{u}, p, g) h^2, \quad (4.38)$$

$$\int_0^T \|\phi - \phi_h\|_h d\tau \leq C(\phi, \phi_t, \mathbf{f}, \mathbf{u}, p, g) h, \quad (4.39)$$

$$\|\mathbf{u}(t) - \mathbf{u}_h(t)\|_{0,\Omega} \leq C(\phi, \phi_t, \mathbf{f}, \mathbf{u}, p, g) h^2, \quad (4.40)$$

$$\|\mathbf{u}(t) - \mathbf{u}_h(t)\|_h + \|p(t) - p_h(t)\|_{0,\Omega} \leq C(\phi, \phi_t, \mathbf{f}, \mathbf{u}, p, g) h. \quad (4.41)$$

PROOF. (4.38) and (4.39) follow by combining the estimates given in (4.27), (4.28) and Lemma 4.7 whereas (4.40) and (4.41) directly follow from (4.38),(4.39) and Lemma 4.3.

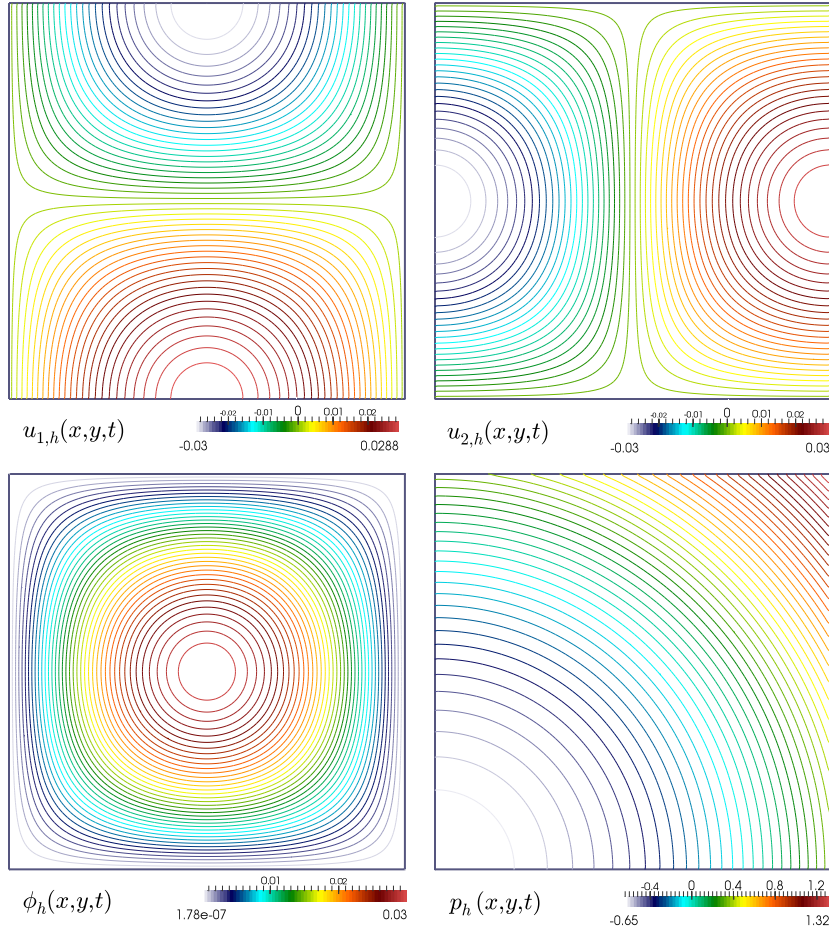


Figure 2: Example 1: Contour plots of the discontinuous finite volume element approximations of velocity components (top panels), and concentration and pressure fields (bottom panels) at the time instant $t = 1$.

5. Numerical examples

We now present a series of numerical tests confirming the convergence rates predicted in Section 4 and simulating some interesting scenarios from the applicative viewpoint. The system of nonlinear equations (3.8)-(3.10) is solved via the Newton-Raphson method with a tolerance of $1e-8$ for the energy norm of the residual, and the associated linear systems are solved with the UMFPAK method [14]. The specific form of the linearized problem is postponed to the Appendix. The penalty parameters are set as $\alpha_c = 1e - 6$, $\alpha_d = 1e3$.

5.1. Example 1: experimental order of convergence against a manufactured exact solution

In Example 1 the ingredients of (2.1) are chosen in such a way that an exact solution is known. To this end, we choose $\kappa(\phi) = \phi^3(1 - \phi/2)^2$, $\mu(\phi) = (1 - \phi/2)^{-2}$, and consider the non-homogeneous problem resulting from adding a non-zero datum \mathbf{j} on the right hand side of the momentum equation of (2.1). The spatial domain is $\Omega = (0, 1)^2$, and the source terms f (which replaces $\nabla \cdot \mathbf{f}(\phi)$) and \mathbf{j} are constructed so that its solution is given by the smooth functions

$$\mathbf{u}(x, y, t) = \begin{pmatrix} \sin(\pi x) \cos(\pi y) \sin(t) \\ -\cos(\pi x) \sin(\pi y) \sin(t) \end{pmatrix}, \quad p(x, y, t) = (x^2 + y^2 - 2/3) \cos(t),$$

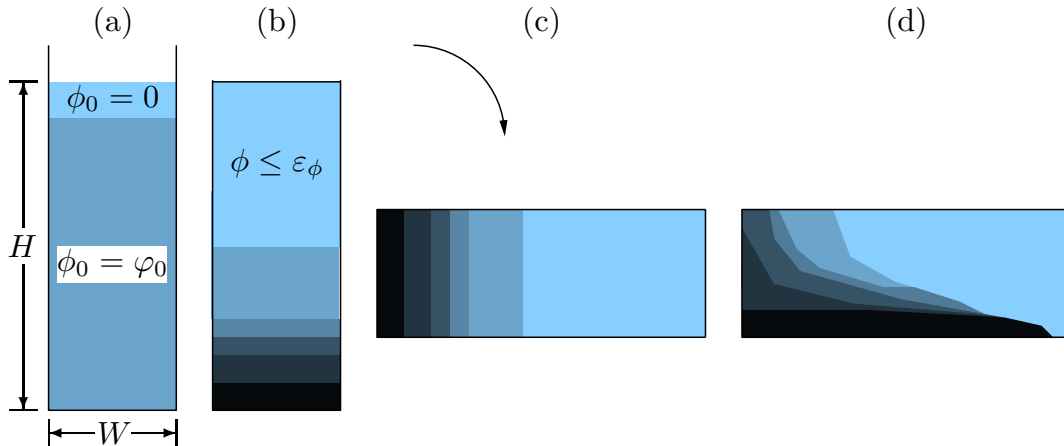


Figure 3: Example 2: spreading of a gravity current [34]. (a) Initial state (not to scale). (b) Once the concentration values in the lower half of the vessel are larger than ε_ϕ , the vessel is tilted. (c) Tilted vessel, (d) gravity current.

$$\phi(x, y, t) = \sin(\pi x) \sin(\pi y) \sin(t).$$

Dirichlet boundary and initial conditions are chosen accordingly to these solutions. We first apply the proposed FVE method on meshes obtained by successive subdivision of Ω into quasi-uniform triangulations \mathcal{T}_h of meshsizes $h = \frac{1}{5}2^{-k}$, with $0 \leq k \leq 6$. For consistence with the analysis in the previous sections, we do not address here the convergence of the time discretization of $(0, T)$, and we simply employing a first order backward Euler formula with a fixed time step $\Delta t = 0.01$, evolving the system until $T = 1$. The approximate solutions obtained on the refinement level $k = 6$ are displayed in Figure 2.

Individual errors in different norms are defined as

$$\begin{aligned} e_0(\mathbf{u}) &= \|\mathbf{u}(t^{N_T}) - \mathbf{u}_h(t^{N_T})\|_{0,\Omega}, \quad e_h(\mathbf{u}) = \|\mathbf{u}(t^{N_T}) - \mathbf{u}_h(t^{N_T})\|_h, \\ e_0(p) &= \|p(t^{N_T}) - p_h(t^{N_T})\|_{0,\Omega}, \quad e_h(\phi) = \|\phi(t^{N_T}) - \phi_h(t^{N_T})\|_h, \quad e_0(\phi) = \|\phi(t^{N_T}) - \phi_h(t^{N_T})\|_{0,\Omega}. \end{aligned}$$

As expected, we observe in Table 1 a convergence of order h^2 for $e_0(\mathbf{u}(t))$ and $e_0(\phi(t))$, an order h for the other spatial errors in their respective norms. An experimental convergence of order Δt (not shown here) has been also observed for all variables in the $\ell^\infty(0, t; L^2(\Omega))$ -norm. An average iteration count (through all refinement levels and time steps) of six Newton steps to achieve the imposed tolerance has been evidenced.

5.2. Example 2: spreading of a suspension gravity current

In this test we are interested in recovering the flow patterns of an experiment carried out in [34]. It consists in a scenario where a rectangular vessel is initially placed vertically, and two separate zones with clear and average concentration are present, and an inflow velocity of normal $\mathbf{u} \cdot \mathbf{n} = u_{\text{in}}$ is imposed at the inlet, located at the bottom of the domain (see the sketch provided in Figure 3). Next, the system evolves and from $t > 0$ to $t = T^*$ three separate zones of clear, mid, and packed sediment are notoriously present, and the inflow velocity is still imposed at the inlet. Suddenly, at $t = T^*$ (which corresponds to a time when a jamming concentration $\varepsilon_\phi = 0.475$ is attained at the bottom of the vessel), the inflow is stopped and the gravity direction is switched -90 degrees, and from $t = T^*$ to $t = T$, one observes the resulting mixing patterns.

The domain is a rectangle of width $W = 50$ and height $H = 500$, and the initial distribution of the concentration is $\phi_0 = 0.4(H - y)^2/H^2$. Zero-flux boundary conditions are considered for ϕ everywhere

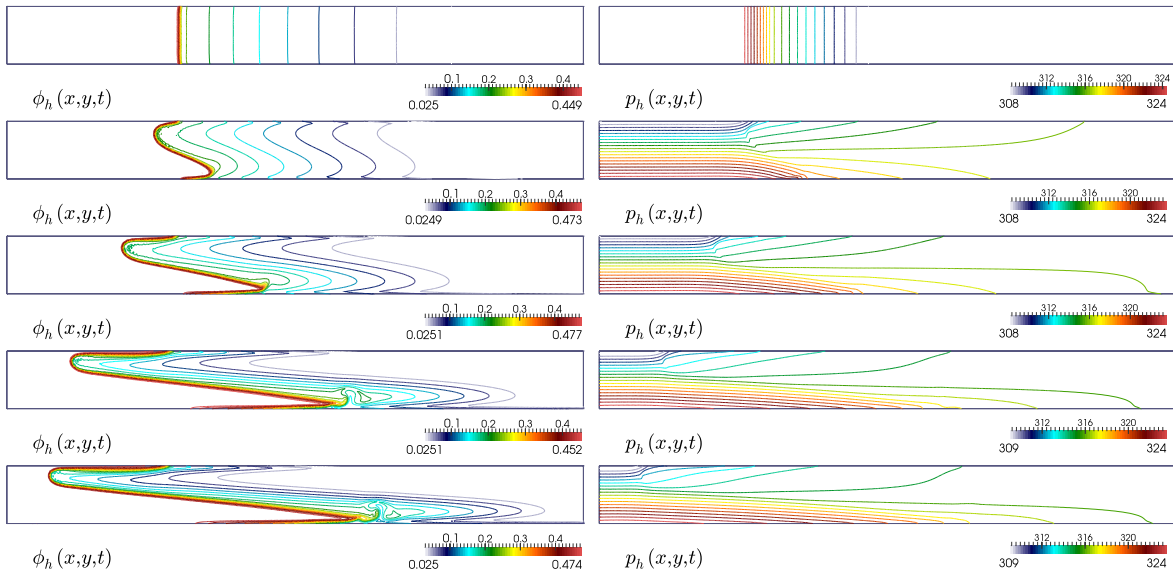


Figure 4: Example 2: Contour plots of the discontinuous finite volume element approximations of concentrations and pressures at time instants $t = 1000, 4000, 8000, 16000, 20000$.

and no-slip data for \mathbf{u} on the top, left, and right boundaries. For this problem we do not consider the effect of sediment compression and so we take $\kappa = D_0$. Instead of $\phi\mathbf{g}$, in this case the forcing term acting on the momentum equation is considered as

$$\frac{\Delta\rho\phi}{(1-\phi)\rho_f + \phi\rho_s}\mathbf{g},$$

and the remaining model parameters are chosen as follows $\beta = 5$, $\tilde{\phi}_{\max} = 0.6$, $u_{\text{in}} = 1.58\text{e-}3$, $D_0 = 1\text{e-}3$, $T^* = 1500$, $\rho_f = 2500$, $g = 1.0$, $\Delta\rho = 1300$. A mesh of 51108 primal cells and 25555 vertices and a timestep of $\Delta t = 0.05$ are employed in the simulations. Figure 4 shows the concentration profiles and pressure distribution during a transient simulation (for visualization purposes the tank is rendered already tilted), whereas Figure 5 depicts contour plots of the associated velocity components.

5.3. Example 3: simulation of an axisymmetric secondary settling tank

Let us now turn to the simulation of the sedimentation process of a zeolites suspension taking place in a secondary clarifier located in the Eindhoven WWTP [36]. Since the vessel and the expected flow patterns are intrinsically axisymmetric, we can restrict the study to a half cross-section of the tank. The axisymmetric domain to consider is presented in Figure 6, along with its dimensions and different parts of its boundary. Notice that such a configuration requires some modifications to the continuous and discrete formulations of the model problem, in particular, all differential operators, infinite and finite-dimensional functional spaces need to be accommodated to the axisymmetric case. A summary of these ingredients is collected in Appendix B, and we refer the reader to e.g. [7] for further details.

The meridional domain Ω sketched in Figure 6 was discretized using an unstructured primal mesh of 96772 triangular elements and 48387 vertices. A fixed timestep of $\Delta t = 3$ s was employed and the system was evolved until $T = 120000$ s. The suspension fed through Γ_{in} with velocity $\mathbf{u}_{\text{in}} = (0, 0.17)^T$ has a concentration of $\phi_{\text{in}} = 0.08$. The material is removed with a constant velocity $\mathbf{u}_{\text{in}} = (0, -0.0000015)^T$ through Γ_{out} , and a constant pressure profile is imposed at the overflow Γ_{off} . In all remaining parts of the boundary we impose zero-flux boundary conditions for the concentration and, except for the

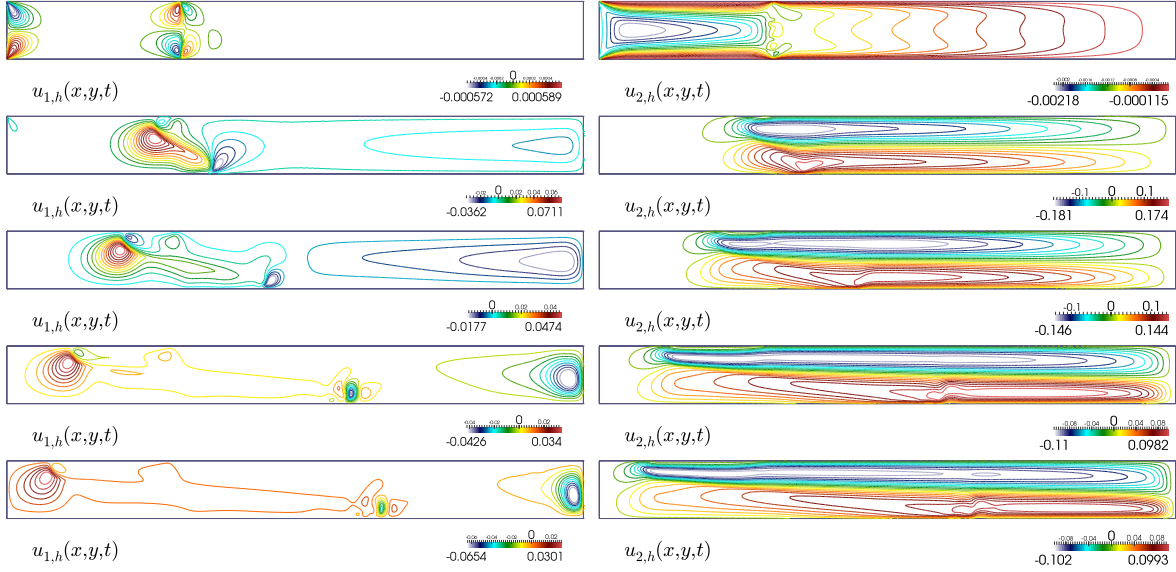


Figure 5: Example 2: Contour plots of the discontinuous finite volume element approximations of velocity components at time instants $t = 1000, 4000, 8000, 16000, 20000$.

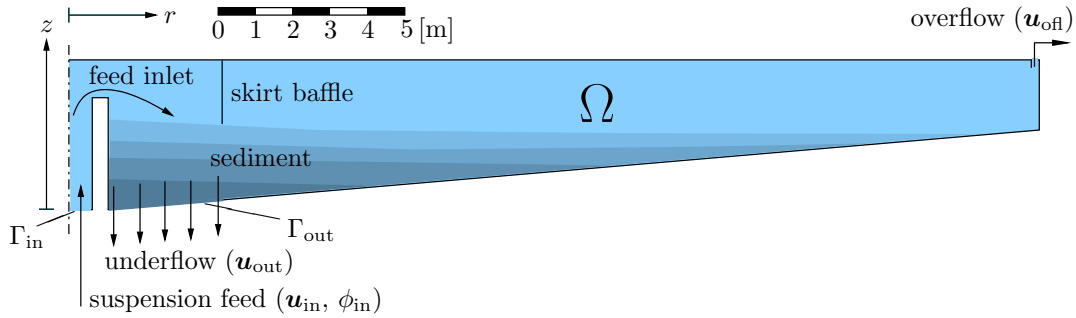


Figure 6: Example 3: secondary settling tank [36]. The device has a feed inlet, a radial underflow for the discharge of sediment, and a peripheral overflow. The variables prescribed on the portions Γ_{in} , Γ_{out} and Γ_{ofl} of the boundary of the (r, z) -domain $\Omega \subset \mathbb{R}^2$ are indicated. The device has a radial length and height of 26 m and 4 m, respectively. The inlet, Γ_{in} , is a horizontal disk of radius 0.6 m. The underflow opening corresponds to the zone from $r = 1.05$ m to $r = 4.1$ m of the conical bottom. The overflow channel corresponds to the annulus between $r = 25.8$ m and $r = 26$ m at $z = 4$ m. The skirt baffle is a thin solid wall reaching from $z = 2.3$ m to $z = 4$ m at $r = 4.1$ m.

symmetry axis, we set no-slip velocities everywhere on $\partial\Omega$. Other functions and parameters are set as $\sigma_e(\phi) = (\sigma_0\alpha/\phi_c^\alpha)\phi^{\alpha-1}$, $\sigma_0 = 0.22$, $\alpha = 5$, $\beta = 2.5$, $\rho_f = 998.2$, $\rho_s = 1750$, $\phi_c = 0.014$, $\tilde{\phi}_{\text{max}} = 0.95$, $v_\infty = 0.0028935$, $g = 9.8$, and $D_0 = v_\infty$.

Snapshots of the approximate solutions computed on the axisymmetric domain are presented in Figures 7 and 8. For visualization purposes, we also depict a rotational extrusion of 330 degrees at the final time 120000 s in Figure 9.

5.4. Example 4: settling in an inclined cylinder

The settling velocity of solid particles within a tilted vessel is known to be accelerated with respect to that in vertical walls. In our last example we study this phenomenon, commonly known as the Boycott effect, where we also test our three-dimensional DFVE implementation. The flow conditions

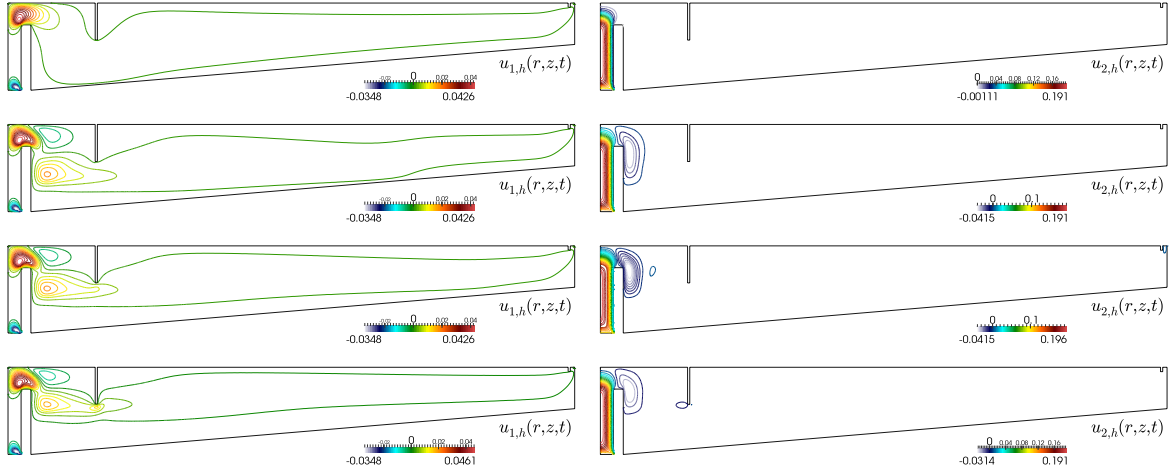


Figure 7: Example 3: Contour plots of the discontinuous finite volume element approximations of velocity components at the time instants $t = 100, 5000, 50000, 100000$ s.

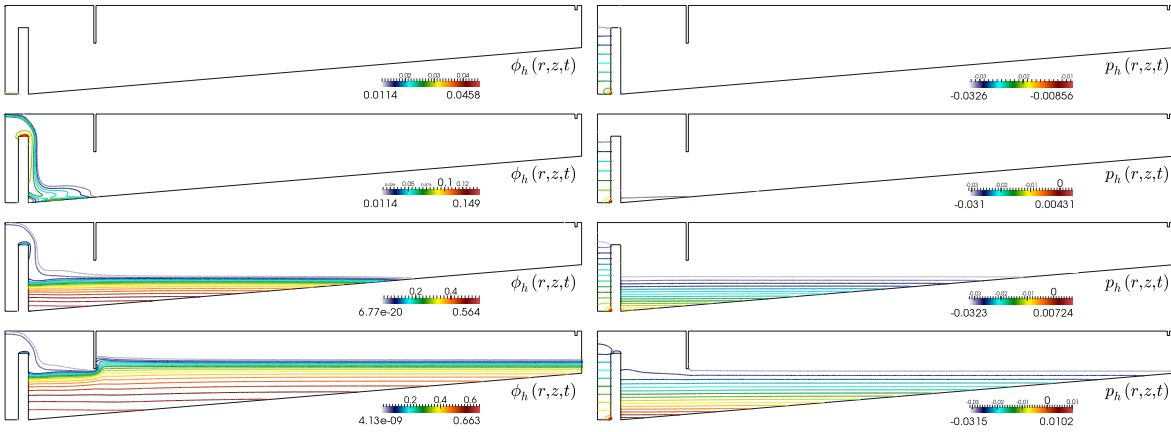


Figure 8: Example 3: Contour plots of the discontinuous finite volume element approximations of concentration (left panels) and pressure field (right plots) at time instants $t = 100, 5000, 50000, 100000$ s.

are assumed as in Example 3, and the computational domain consists of a tilted cylinder of height 8m and radius 2m, forming an angle of $\pi/4$ with the y -axis. The concentration-dependent viscosity is given by (2.4) with $\hat{\phi}_{\max} = 0.85$ and $\beta = 2$. An unstructured mesh of 48361 vertices and 267297 tetrahedral primal elements has been generated to discretize the domain. We employ a timestep of $\Delta t = 0.01$ and evolve the system until $T = 16$. We study the elementary batch-sedimentation case, therefore no-flux boundary conditions for the concentration, and no-slip velocities are set on the whole boundary. Three snapshots of the approximate solutions are displayed in Figure 10.

Acknowledgments

The authors wish to thank Elena Torfs (Ghent University) for providing the measures of the geometry and expected flow conditions addressed in Section 5.3. In addition, RB is supported by Fondecyt project 1130154; BASAL project CMM, Universidad de Chile and Centro de Investigación

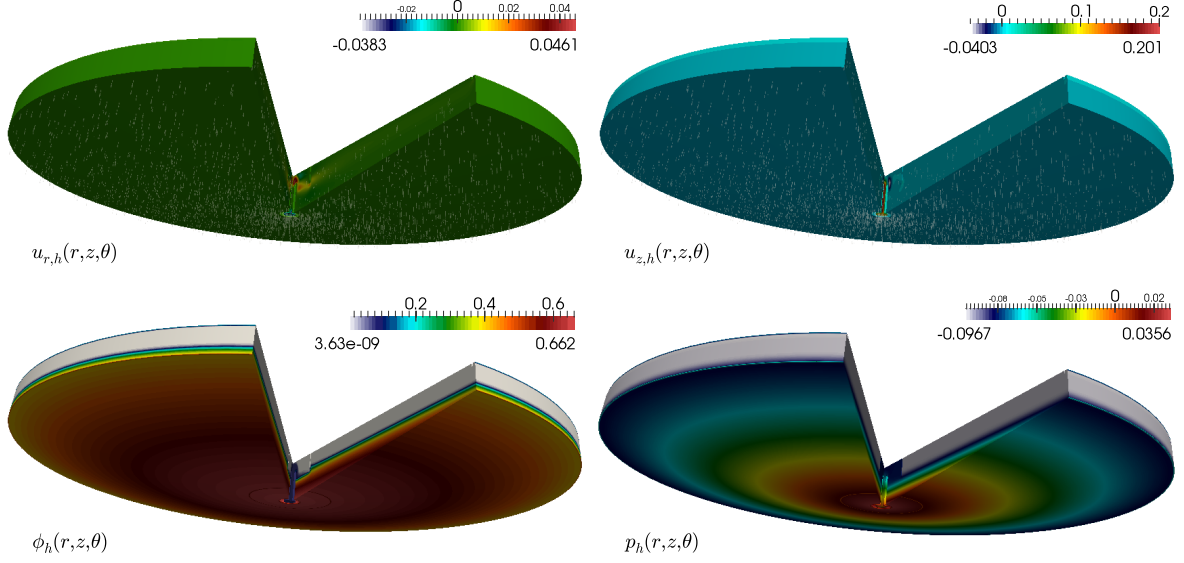


Figure 9: Example 3: Rotational extrusion of the discontinuous finite volume element approximations of velocity components, concentration, and pressure at time $t = 120000$ s.

en Ingeniería Matemática (CI²MA), Universidad de Concepción; Conicyt project Anillo ACT1118 (ANANUM); Red Doctoral REDOC.CTA, MINEDUC project UCO1202; and CRHIAM, project CONICYT/FONDAP/15130015. SK is thankful to CI²MA, Universidad de Concepción for providing financial support for a short term visit to that center, where the present work was substantially advanced. The work of RRB was supported by the Swiss National Science Foundation through the research grant PP00P2-144922.

A. Newton linearization

We apply a first-order backward Euler time stepping. For a fixed time $t = t^n < T$, we denote by $(\delta\phi_h^k, \delta\mathbf{u}_h^k, \delta p_h^k)$ an increment of the state $(\phi_h^k, \mathbf{u}_h^k, p_h^k)$ for $k = 1, \dots, k_{\max}$. This increment is the solution of the following linearization of (3.8)–(3.10):

$$\begin{aligned}
& \frac{1}{\Delta t} \langle \delta\phi_h^k, \mathcal{R}^\# \varphi_h \rangle + \mathcal{A}(\delta\phi_h^k, \varphi_h, \phi_h^k) + \int_{\Omega} \kappa'(\phi_h^k) \delta\phi_h^k \nabla \phi_h^k \cdot \nabla \varphi_h \, dx + \mathcal{C}(\phi_h^k, \varphi_h, \delta\mathbf{u}_h^k) + \mathcal{C}(\delta\phi_h^k, \varphi_h, \mathbf{u}_h^k) \\
& = -\frac{1}{\Delta t} \langle \phi_h^k, \mathcal{R}^\# \varphi_h \rangle - \mathcal{A}(\phi_h^k, \varphi_h, \phi_h^k) - \mathcal{C}(\phi_h^k, \varphi_h, \mathbf{u}_h^k) + \langle f, \varphi_h \rangle + \frac{1}{\Delta t} \langle \phi_h^{n-1}, \mathcal{R}^\# \varphi_h \rangle, \\
& \hat{A}(\delta\mathbf{u}_h^k, \mathbf{v}_h; \phi_h^k) + \int_{\Omega} \mu'(\phi_h^k) \delta\phi_h^k \varepsilon(\mathbf{u}_h^k) : \varepsilon(\mathbf{v}_h) \, dx - b(\delta p_h^k, \mathbf{v}_h) - d(\delta\phi_h^k, \mathcal{P}^\# \mathbf{v}_h) \\
& = -\hat{A}(\mathbf{u}_h^k, \mathbf{v}_h; \phi_h^k) + b(p_h^k, \mathbf{v}_h) + d(\phi_h^k, \mathcal{P}^\# \mathbf{v}_h) + \langle \mathbf{j}, \mathbf{v}_h \rangle, \\
& b(q_h, \delta\mathbf{u}_h^k) + b(q_h, \mathbf{u}_h^k) = 0,
\end{aligned} \tag{A.1}$$

for all $(\varphi_h, \mathbf{v}_h, q_h) \in \mathcal{S}_h \times \mathcal{V}_h \times \mathcal{Q}_h$, associated to homogeneous Dirichlet boundary conditions for the increment of velocity and concentration. The state at step k is assumed to satisfy the nonhomogeneous boundary datum imposed with the initial condition, and the overall loop is summarized in Algorithm 1.

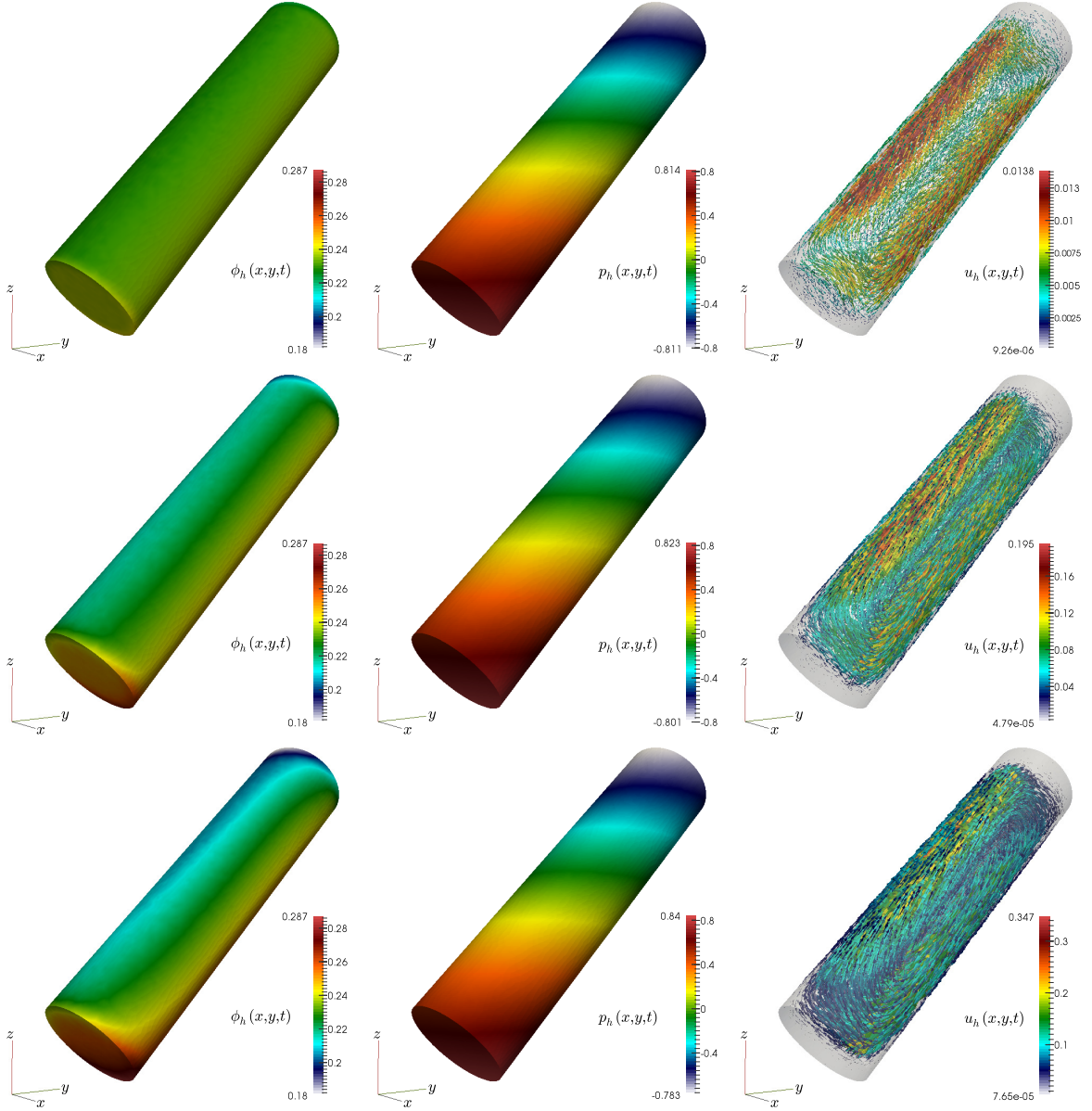


Figure 10: Example 4: Discontinuous finite volume element approximations of concentration (left panels), pressure field (center), and velocity vectors (right) for the batch sedimentation process in a tilted cylinder. Snapshots at time instants $t = 5, 10, 16$ s (top, middle, and bottom, respectively).

B. Axisymmetric formulation for the sedimentation problem

Let $d = 3$. Under the assumption of cylindrical symmetry (with respect to the symmetry axis $\Gamma_s = \{r = 0\}$, cf. Figure 6) of all the flow patterns, the expected concentration profiles, and the domain, the three-dimensional problem (2.1) in Cartesian coordinates (x, y, z, t) can be recast as the following two-dimensional system written in cylindrical coordinates (r, z, t) :

For all $t > 0$, find $\mathbf{u}(t) \in V_{1,\Gamma_s}^1(\Omega) \times H_{1,\Gamma}^1(\Omega)$, $p(t) \in L_{1,0}^2(\Omega)$ and $\phi(t) \in H_1^1(\Omega)$ such that

$$\partial_t \phi - \operatorname{div}_a(\kappa(\phi) \nabla_a \phi) + \mathbf{u} \cdot \nabla_a \phi = \nabla_a \cdot \mathbf{f}(\phi) \quad \text{in } \Omega \times (0, T),$$

Algorithm 1 Solution algorithm

- 1: Construct primal and dual meshes, set initial conditions ϕ_h^0 , Newton tolerance ϵ , and global time step Δt
- 2: **for** $n = 1, \dots, N$ **do**
- 3: set initial guess $\phi_h^{k=0} \leftarrow \phi_h^{n-1}$, $\mathbf{u}_h^{k=0} \leftarrow \mathbf{u}_h^{n-1}$, $p_h^{k=0} \leftarrow 0$
- 4: reset the norm of the increment $\epsilon_R^{k=0} \leftarrow 2\epsilon$
- 5: **for** $k = 1, \dots, k_{\max}$ **do**
- 6: given the values $(\phi_h^k, \mathbf{u}_h^k, p_h^k)$, find the increments $(\delta\phi_h^k, \delta\mathbf{u}_h^k, \delta p_h^k)$ by solving (A.1)
- 7: Compute the energy norm of the increment

$$\epsilon_R^k \leftarrow (\|\delta\phi_h^k\|_{1,\Omega}^2 + \|\delta\mathbf{u}_h^k\|_h^2 + \|\delta p_h^k\|_{0,\Omega}^2)^{1/2}$$

- 8: Update the value of the approximation

$$\phi_h^n \leftarrow \delta\phi_h^k + \phi_h^k, \quad \mathbf{u}_h^n \leftarrow \delta\mathbf{u}_h^k + \mathbf{u}_h^k, \quad p_h^n \leftarrow \delta p_h^k + p_h^k$$

- 9: **if** $\epsilon_R^k < \epsilon$ **or** $k \geq k_{\max}$ **then**
 - 10: break
 - 11: **else**
 - 12: continue
 - 13: **end if**
 - 14: **end for**
 - 15: **end for**
-

$$\begin{aligned} -\operatorname{div}_a(\mu(\phi)\boldsymbol{\varepsilon}_a(\mathbf{u}) - p\mathbf{I}) - \phi\mathbf{g} &= \mathbf{0} && \text{in } \Omega \times (0, T), \\ \operatorname{div}_a \mathbf{u} &= 0 && \text{in } \Omega \times (0, T), \\ \mathbf{u} &= \mathbf{u}_\Gamma && \text{on } \Gamma \times (0, T), \\ \phi &= \phi_\Gamma && \text{on } \Gamma \times (0, T), \\ \phi(0) &= \phi_0 && \text{on } \Omega \times \{0\}. \end{aligned}$$

Here the involved modified spaces are defined as follows (see details in e.g. [29, 7, 2]):

$$\begin{aligned} V_1^1(\Omega) &:= H_1^1(\Omega) \cap L_{-1}^2(\Omega), \quad V_{1,\Gamma_s}^1(\Omega) := \{w \in V_1^1(\Omega) : w = 0 \text{ on } \Gamma_s\}, \\ L_{1,0}^2(\Omega) &:= \left\{ q \in L_1^2(\Omega) : \int_\Omega q r \, dr \, dz = 0 \right\}, \end{aligned}$$

where $L_\alpha^p(\Omega)$ denotes the space of measurable functions v on Ω such that

$$\|v\|_{L_\alpha^p(\Omega)}^p := \int_\Omega |v|^p r^\alpha \, dr \, dz < \infty,$$

$H_\alpha^m(\Omega)$ is the space of functions in $L_\alpha^p(\Omega)$ with derivatives up to order m also in $L_\alpha^p(\Omega)$, and $H_{\alpha,\Gamma}^m(\Omega)$ denotes its restriction to functions with null trace on a part of the boundary Γ . The modified differential operators are defined as

$$\nabla_a \mathbf{v} := \begin{bmatrix} \partial_r v_r & \partial_r v_z \\ \partial_z v_r & \partial_z v_z \end{bmatrix}, \quad \operatorname{div}_a \mathbf{v} := \partial_z v_z + \frac{1}{r} \partial_r (r v_r), \quad \boldsymbol{\varepsilon}_a(\mathbf{v}) := \frac{1}{2} (\nabla_a \mathbf{v} + \nabla_a \mathbf{v}^T), \quad \nabla_a s = \begin{pmatrix} \partial_r s \\ \partial_z s \end{pmatrix}.$$

Moreover, all volume integrals in the definition of the DVFE formulation (3.8)-(3.10) have been replaced by their weighted counterparts, and the discrete spaces have been replaced by

$$\mathbf{V}_h^a := \{ \mathbf{v} \in V_1^1(\Omega) \times V_{1,\Gamma_s}^1(\Omega) : \mathbf{v}|_K \in \mathbb{P}_1(K)^d, \forall K \in \mathcal{T}_h \},$$

$$\mathcal{Q}_h^a := \{q \in L_{1,0}^2(\Omega) : q|_K \in \mathbb{P}_0(K), \forall K \in \mathcal{T}_h\},$$

$$\mathcal{S}_h^a := \{\varphi \in L_1^2(\Omega) : \varphi|_K \in \mathbb{P}_1(K), \forall K \in \mathcal{T}_h\}.$$

References

- [1] S. Agmon, Lectures on Elliptic Boundary Value Problems, AMS, Providence, Rhode Island, 2010.
- [2] V. Anaya, D. Mora, C. Reales, R. Ruiz-Baier, Stabilized mixed finite element approximation of axisymmetric Brinkman flows, CI²MA preprint 2014-19. Available from <http://www.ci2ma.udec.cl/publicaciones/prepublicaciones>.
- [3] D. N. Arnold, An interior penalty finite element method with discontinuous elements, SIAM J. Numer. Anal. 19 (1982) 724–760.
- [4] C. Bi, M. Liu, A discontinuous finite volume element method for second-order elliptic problems, Numer. Meth. Part. Diff. Eqns. 28 (2012) 425–440.
- [5] R. Bürger, S. Diehl, Convexity-preserving flux identification for scalar conservation laws modelling sedimentation, Inverse Problems 29 (2013) paper 045008 (30pp).
- [6] R. Bürger, S. Diehl, I. Nopens, E. Torfs, A consistent modelling methodology for secondary settling tanks: a reliable numerical method, Water Sci. Tech. 68 (2013) 192–208.
- [7] R. Bürger, R. Ruiz-Baier, H. Torres, A stabilized finite volume element formulation for sedimentation-consolidation processes, SIAM J. Sci. Comput. 34 (2012) B265–B289.
- [8] R. Bürger, W.L. Wendland, F. Concha, Model equations for gravitational sedimentation-consolidation processes, ZAMM Z. Angew. Math. Mech. 80 (2000) 79–92.
- [9] Z. Cai, On the finite volume element method. Numer. Math. 58 (1991) 713–735.
- [10] P. Chatzipantelidis, V. Ginting, A finite volume element method for a nonlinear parabolic problem. In: O.P. Iliev, S.D. Margenov, P.D. Minev, P.S. Vassilevski and L.T. Zikatanov (Eds.), Numerical Solution of Partial Differential Equations: Theory, Algorithms, and Their Applications. Springer, New York, 121–136, 2013.
- [11] P. Chatzipantelidis, V. Ginting, R.D. Lazarov, A finite volume element method for a nonlinear elliptic problem, Numer. Lin. Alg. Appl. 12 (2005) 515–546.
- [12] S.C. Chou, Analysis and convergence of a covolume method for the generalized Stokes problem. Math. Comp. 66 (1997) 85–104.
- [13] M. Cui, X. Ye, Unified analysis of finite volume methods for the Stokes equations, SIAM J. Numer. Anal. 48 (2010) 824–839.
- [14] T.A. Davis, An unsymmetric-pattern multifrontal method for sparse LU factorization, SIAM J. Matrix Anal. Appl. 18 (1997) 140–158.
- [15] G.A. Ekama, J.L. Barnard, F.W. Günthert, P. Krebs, J.A. McCorquodale, D.S. Parker, E.J. Wahlberg, Secondary Settling Tanks: Theory, Modelling, Design and Operation. Scientific and Technical report 6, International Association on Water Quality, London, 1997.
- [16] A. Guardone, L. Vigevano, Finite element/volume solution to axisymmetric conservation laws, J. Comput. Phys. 224 (2007) 489–518.
- [17] E. Guazzelli, J. Hinch, Fluctuations and instability in sedimentation, Annu. Rev. Fluid Mech. 43 (2011) 97–116.

- [18] E. Guazzelli, J.E. Morris, *A Physical Introduction to Suspension Dynamics*, Cambridge University Press, 2012.
- [19] T. Gudi, N. Nataraj, A.K. Pani, hp-Discontinuous Galerkin methods for strongly nonlinear elliptic boundary value problems, *Numer. Math.* 109 (2008) 233–268.
- [20] S. Kumar, A mixed and discontinuous Galerkin finite volume element method for incompressible miscible displacement problems in porous media, *Numer. Meth. Partial Diff. Eqns.* 28 (2012) 1354–1381.
- [21] S. Kumar, On the approximation of incompressible miscible displacement problems in porous media by mixed and standard finite volume element methods, *Int. J. Model. Simul. Sci. Comput.* 4 (2013), paper 1350013 (30pp).
- [22] S. Kumar, N. Nataraj, A.K. Pani, Discontinuous Galerkin finite volume element methods for second order linear elliptic problems, *Numer. Meth. Part. Diff. Eqns.* 25 (2009) 1402–1424.
- [23] S. Kumar, R. Ruiz-Baier, Equal order discontinuous finite volume element methods for the Stokes problem, *J. Sci. Comput.*, submitted.
- [24] G.J. Kynch, A theory of sedimentation, *Trans. Farad. Soc.* 48 (1952) 166–176.
- [25] R.H. Li, Generalized difference methods for a nonlinear Dirichlet problem, *SIAM J. Numer. Anal.* 24 (1987) 77–88.
- [26] J. Li and Z. Chen, A new stabilized finite volume method for the stationary Stokes equations, *Adv. Comput. Math.* 30 (2009) 141–152.
- [27] S.A. Lorca, J.L. Boldrini, The initial value problem for a generalized Boussinesq model, *Nonlin. Anal.* 36 (1999) 457–480.
- [28] Z. Luo, H. Li, P. Sun, A fully discrete stabilized mixed finite volume element formulation for the non-stationary conduction-convection problem, *J. Math. Anal. Appl.* 404 (2013) 71–85.
- [29] B. Mercier, G. Raugel, Resolution d’un problème aux limites dans un ouvert axisymétrique par éléments finis en r , z et séries de Fourier en t , *RAIRO Anal. Numér.* 16 (1982) 405–461.
- [30] M.R. Ohm, H.Y. Lee, J.Y. Shin, Error estimates for discontinuous Galerkin methods for nonlinear parabolic problems, *J. Math. Anal. Appl.* 315 (2006) 132–143.
- [31] A. Quarteroni, R. Ruiz-Baier, Analysis of a finite volume element method for the Stokes problem, *Numer. Math.* 118 (2011) 737–764.
- [32] J.F. Richardson, W.N. Zaki, Sedimentation and fluidization: Part I, *Trans. Instn. Chem. Engrs. (London)* 32 (1954) 35–52.
- [33] R. Ruiz-Baier, H. Torres, Numerical solution of a coupled flow-transport system modeling multi-dimensional sedimentation processes, *Appl. Numer. Math.*, in press.
- [34] S. Saha, D. Salin, L. Talon, Low Reynolds number suspension gravity currents, *Eur. J. Phys. E* 36 (2013), paper 85 (18pp.)
- [35] S. Sun, B. Rivière, M.F. Wheeler, A combined mixed finite element and discontinuous Galerkin method for miscible displacement problem in porous media, in: T.F. Chan, Y. Huang, T. Tang, J. Xu, L.-A. Ying (Eds), *Recent Progresses in Computational and Applied PDEs, Proceedings of the International Conference, Zhangjiajie, July 2001*. Kluwer Academic/Plenum Publishers, New York, 321–348, 2002.
- [36] E. Torfs (Ghent University). Private communication.

- [37] M. Ungarish, *An Introduction to Gravity Currents and Intrusions*. CRC Press, Boca Raton, FL, 2009.
- [38] J. Wen, Y. He, J. Yang, Multiscale enrichment of a finite volume element method for the stationary Navier–Stokes problem. *Int. J. Comput. Math.* 90 (2013) 1938–1957.
- [39] B.A. Wills, T. Napier-Munn, *Wills Mineral Processing Technology*, seventh ed. Butterworth-Heinemann/Elsevier, Oxford, UK, 2006.
- [40] Q. Yang, Z. Jiang, A discontinuous mixed covolume method for elliptic problems, *J. Comput. Appl. Math.* 235 (2011) 2467–2476.
- [41] X. Ye, A new discontinuous finite volume method for elliptic problems, *SIAM J. Numer. Anal.* 42 (2004) 1062–1072.
- [42] X. Ye, A discontinuous finite volume method for the Stokes problem, *SIAM J. Numer. Anal.* 44 (2006) 183–198.

Centro de Investigación en Ingeniería Matemática (CI²MA)

PRE-PUBLICACIONES 2014

- 2014-14 FABIÁN FLORES-BAZÁN, NICOLÁS HADJISAVVAS, FELIPE LARA: *Second order asymptotic analysis: basic theory*
- 2014-15 ANAHI GAJARDO, CAMILO LACALLE: *Revisiting of 2-pebble automata from a dynamical approach*
- 2014-16 MUHAMMAD FARYAD, AKHLESH LAKHTAKIA, PETER MONK, MANUEL SOLANO: *Comparison of rigorous coupled-wave approach and finite element method for photovoltaic devices with periodically corrugated metallic backreflector*
- 2014-17 STEFAN BERRES, ANÍBAL CORONEL, RICHARD LAGOS, MAURICIO SEPÚLVEDA: *Numerical calibration of scalar conservation law models using real coded genetic algorithm*
- 2014-18 JESSIKA CAMAÑO, GABRIEL N. GATICA, RICARDO OYARZÚA, RICARDO RUIZ-BAIER, PABLO VENEGAS: *New fully-mixed finite element methods for the Stokes-Darcy coupling*
- 2014-19 VERONICA ANAYA, DAVID MORA, CARLOS REALES, RICARDO RUIZ-BAIER: *Stabilized mixed finite element approximation of axisymmetric Brinkman flows*
- 2014-20 VERONICA ANAYA, DAVID MORA, RICARDO OYARZÚA, RICARDO RUIZ-BAIER: *A priori and a posteriori error analysis for a vorticity-based mixed formulation of the generalized Stokes equations*
- 2014-21 SALIM MEDDAHI, DAVID MORA: *Nonconforming mixed finite element approximation of a fluid-structure interaction spectral problem*
- 2014-22 EDUARDO LARA, RODOLFO RODRÍGUEZ, PABLO VENEGAS: *Spectral approximation of the curl operator in multiply connected domains*
- 2014-23 GABRIEL N. GATICA, FILANDER A. SEQUEIRA: *Analysis of an augmented HDG method for a class of quasi-Newtonian Stokes flows*
- 2014-24 MARIO ÁLVAREZ, GABRIEL N. GATICA, RICARDO RUIZ-BAIER: *An augmented mixed-primal finite element method for a coupled flow-transport problem*
- 2014-25 RAIMUND BÜRGER, SARVESH KUMAR, RICARDO RUIZ-BAIER: *Discontinuous finite volume element discretization for coupled flow-transport problems arising in models of sedimentation*

Para obtener copias de las Pre-Publicaciones, escribir o llamar a: DIRECTOR, CENTRO DE INVESTIGACIÓN EN INGENIERÍA MATEMÁTICA, UNIVERSIDAD DE CONCEPCIÓN, CASILLA 160-C, CONCEPCIÓN, CHILE, TEL.: 41-2661324, o bien, visitar la página web del centro: <http://www.ci2ma.udec.cl>



**CENTRO DE INVESTIGACIÓN EN
INGENIERÍA MATEMÁTICA (CI²MA)
Universidad de Concepción**



Casilla 160-C, Concepción, Chile
Tel.: 56-41-2661324/2661554/2661316
<http://www.ci2ma.udec.cl>

